Wavelet Transform Applications (i) Voltage Envelope Detection and (ii) Computation of AM, FM, PM.

A Dissertation submitted towards the partial fulfilment
of the requirement for the award of degree of

Master of Technology
in
Signal Processing & Digital Design

Submitted by

Monika Gupta

2K15/SPD/09

Under the supervision of

Dr. Sudipta Majumdar
(Assistant Professor, Department of ECE)

Department of Electronics & Communication Engineering
Delhi Technological University
(Formerly Delhi College of Engineering)
Delhi-110042
2015-2017

DELHI TECHNOLOGICAL UNIVERSITY

Established by Govt. Of Delhi vide Act 6 of 2009

(Formerly Delhi College of Engineering)

SHAHBAD DAULATPUR, BAWANA ROAD, DELHI-110042

CERTIFICATE

This is to certify that the dissertation entitled "**Wavelet Transform Applications (i) Voltage Envelope Detection and (ii) Computation of AM, FM, PM"** submitted by **Monika Gupta, Roll. No. 2K15/SPD/09**, in partial fulfilment for the award of degree of Master of Technology in "**Signal Processing and Digital Design (SPDD)",** Department of Electronics & Communication Engineering in Delhi Technological University during the year 2015-2017.

Dr. Sudipta Majumdar

Supervisor

Assistant Professor (ECE)

Delhi Technological University

Delhi-110042

DECLARATION

I hereby declare that I have fully cited all materials presented by others which I have used in this thesis. It is being submitted for the degree of Master of Technology in Signal Processing & Digital Design at the Delhi Technological University.

Monika Gupta
M. Tech. (SPDD)

2K15/SPD/09

Date: Nov, 2018

Place: Delhi Technological University, Delhi

ACKNOWLEDGEMENT

I owe my gratitude to all the people who have helped me in this dissertation work and who have made my postgraduate college experience one of the most special periods of my life.

Firstly, I would like to express my deepest gratitude to my supervisor **Dr. Sudipta Majumdar**, Assistant Professor (ECE) for her invaluable support, guidance, motivation and encouragement throughout the period during which this work was carried out. I am deeply grateful to **Dr. S. Indu,** H.O.D. (Deptt. Of E.C.E) for her support and encouragement in carrying out this project.

I also wish to express my heart full thanks to all the faculty at Department of Electronics & Communication Engineering of Delhi Technological University for their goodwill and support that helped me a lot in successful completion of this project.

Finally, I want to thank my parents, family and friends for always believing in my abilities and showering their invaluable love and support.

Monika Gupta

M. Tech. (SPDD)

2K15/SPD/09

Abstract

Estimation of instantaneous features of a signal such as instantaneous frequency, phase, and amplitude is found sensitive in the presence of noise. The instantaneous features of the signal can be calculated using the analytic signal. This work presents two different applications of instantaneous parameters using wavelet transform (1) Detection of instantaneous flicker level using Prony analysis and analytic signal (2) decomposition of amplitude modulated-frequency modulated signal. We propose wavelet transform based analytic signal calculation for the detection of voltage envelope of the flicker and decomposition of amplitude modulation and frequency modulation of time varying sinusoidal model in the presence of white Gaussian noise and compared the results using Hilbert transform based analytic signal calculation. MATLAB simulation results show that analytic signal using wavelet transform performs better in terms of anti noise performance and precision.

Table of **Contents**

CHAPTER 1: INTRODUCTION

1.1 Objective

Estimation of various signal features such as instantaneous frequency, phase, and amplitude of the signal is found sensitive in the presence of noise. This work presents (1) detection of instantaneous flicker level by extracting magnitude, frequency and phase angle by Prony method and (2) computation of frequency, phase and amplitude using vector interpretation of analytic signal. We calculated analytic signal using wavelet based method and implemented for voltage envelope detection and decomposition of AM-FM signal as a vector interpretation of the analytic signal. Then we compared the proposed method for the detection of voltage envelope and decomposition of AM-FM signals using the analytic signal by Hilbert transform [1]-[3].

1.2 Background

Voltage flicker:

Fluctuations of voltage (VF) are the variations of voltage envelope. These variations are random in nature. The unsteadiness in the optical sensation is due to the fluctuations of spectral distributions of the light source. Reciprocating compressors, arc furnaces, and large motors are typical sources of voltage fluctuations. The quality of the energy distributed by power companies are highly affected due to these voltage fluctuations. Thus it is very important to estimate the amplitude and frequency of the voltage flicker waveform. These fluctuations occur when the inter-harmonic components are not synchronous with the component of the fundamental frequency, then the disturbances in peak magnitudes and root mean square magnitude in voltage waveform takes place [4]. This is the reason that voltage flicker envelope is also called as instantaneous flicker level (IFL). The IFL may be comprised of single frequency as well as multiple or band of frequencies.

AM-FM decomposition:

Time-varying models provide higher resolution representation of natural systems/signals than the time-invariant models. Speech/audio signals are common examples of the output of time-varying systems whose subtle variations are perceived and utilized effectively. The human ability to perceive changes in speech/audio signals is remarkable and speech/audio communication are excellent instances of highly evolved systems for communicating information, emotion, entertainment etc. One of the basic models for signals with time-varying properties is in terms of varying amplitude (amplitude modulation (AM) or

envelope) and/or frequency of oscillation (or frequency modulation, FM). Such signals are called AM-FM signals. Extracting the envelope and frequency from such signals is called AM-FM decomposition.

Analytic signal:

Estimation of instantaneous parameters such as instantaneous frequency, instantaneous amplitude, and instantaneous phase is useful in many applications and is still in interest in many areas of research for example in communication systems, seismic signal processing, radar signal processing etc. [5]-[6]. The most commonly used method is Hilbert transform. The analytic signal is formed combining the real valued signal and its corresponding Hilbert transform.

1.2 Organization of The Thesis

The organization of the thesis is as follows:

Chapter 1 provides an introduction to the analytic signal and instantaneous parameter estimation. It also presents a brief introduction to voltage flicker and AM-FM models.

Chapter 2 presents a brief introduction to some recent developments in the measurement of voltage flicker and AM-FM decomposition and its applications.

Chapter 3 presents processing techniques used in this work namely Hilbert transform, continuous wavelet transform, Prony decomposition technique and amplitude modulated-frequency modulated model.

Chapter 4 presents the proposed method for the estimation of voltage envelope of the flicker waveform and decomposition of AM-FM signal with the help of analytic signal constructed using wavelet transform.

Chapter 5 presents implementation and simulation results.

Chapter 6 presents discussion and future scope.

CHAPTER 2: RELATED ARTICLES

Decomposition of AM-FM signal is important for music and speech applications.

In 2004, Li and Atlas [7], proposed the estimation of AM-FM model of the over-modulated signal in a two-step process. The analysis was based on coherent demodulation. The algorithm consists of calculation of conventional AM and FM as the first step. The next step was FM-to-AM transduction block which was followed by a coherent demodulator. The evaluation of source sensitivity for the algorithm showed that the estimation errors generally increase with AM and FM frequencies, but are insensitive to the carrier frequency. The algorithm had a limitation that it does not work properly if the AM is complex.

In 2008, Marco Grimaldi et al. [8], presented parameterization of the speech signal based on the amplitude modulation-frequency modulation model of the speech signal. The parameters were used for the speaker identification. To predict the identity of a speaker different instantaneous frequency were formed by the same AM-FM framework. Three decompositions of the voiced speech were done. The first step followed the method for tracking the speech formants, the second step was to calculate similar resonances below 4 kHz, and the third step was the scaling of the bandwidth. Using all three steps, different parameters were extracted and utilized for identification of the speaker. The results showed the speaker identification using AM-FM models performed better compared to Mel-frequency cepstral coefficients (MFCC) and Gaussian mixture model (GMM) classification system.

In 2014, Arun Venkitaraman et al. [9] presented a method for amplitude modulation and frequency modulation separation using the input signal and its corresponding phase-shifted signal. Two all pass filters were used and the impulse response of all pass filters was related by Fractional Hilbert transform. The all pass filter was formed using cosine modulated flat top low pass filter. The outputs of the two all pass filter were joined together to create an analytic signal. From this analytic signal, the AM and FM were calculated. In this paper, the concept of demodulation of multi component

AM-FM signal using the all pass filter, cosine modulated filterbank and constant Q-filterbank was also considered. The results showed that the cosine modulated filterbank approach performed better as compared to other techniques such as the Gabor's analytic signal approach, the Teager-energy-based approach, and the linear transduction filter approach. One of the disadvantages of this method is the unreliable estimation of the time delays between binaural signals.

In 2015, Parasuraman Sumath et al. [10], proposed a sliding discrete Fourier transform-based PLL (Phase locked loop) to decompose mono component AM-FM signal. It was shown that the sliding DFT filter is prone to windowing effect if input signal frequency drifts from the center carrier frequency. The amplitude errors and the phase errors produced by the windowing effect had been used to gain the lock condition of the PLL. The variation from the center frequency generated phase and magnitude errors in the form of in-phase and quadrature-phase components. The magnitude error was found because of the variations in frequency. To get the corresponding AM, the in phase component was passed to a full wave rectifier. Thus the amplitude and frequency variation of the AM-FM signal was calculated simultaneously. The result showed that the PLL based method could be used to decompose AM-FM signal having large variations in frequency and the amplitude.

In 2015, Haricharan Aragonda et al. [11], proposed an algorithm to separate the amplitude modulation (AM), which corresponds to the response of vocal tract and the frequency modulation (FM) that corresponds to the excitation of the voiced speech. The demodulation algorithm of the AM-FM signal was based on the Riesz transform and Hilbert transform. A comparison had been made between the Riesz transform technique and sinusoidal demodulation technique on real speech data. The results showed that the Riesz-transform based method characterizes the spectrogram more precisely. The signal to noise ratio (SNR) of the reconstructed speech signal was found 2 dB higher using the Riesz transform method.

Voltage flicker analysis is one of the elementary tools for power quality assessment in power systems. Determination of the envelope of voltage flicker is one of the researched fields in signal processing. Various methods have been used to determine voltage flicker.

In 2012, Iman Sadinezhat et al. [12] proposed adaptive Kalman filter and least square algorithm based method to estimate the voltage fluctuations in the power distribution system. A two step model was followed. The extraction of the fundamental frequency component was done by the least square algorithm and the coefficients were updated based on the inter harmonics in the voltage waveform. The second step was to estimate the instantaneous flicker level of the voltage waveform by the Kalman filter. The result showed that the Kalman least square algorithm in the Gaussian noise of 10 dB produced an error of 3.387 for the amplitude estimation and 0.0462 for the frequency estimation.

In 2014, Wenxuan Yao et al. [13] proposed fast S-transform and used it to estimate the components of the time varying flicker. Teager energy operator was also utilized to calculate the characteristics of the flicker. The fast S-transform extracted both the frequency and time domain information of the voltage flicker. It has been shown that the fast S-transform had lower computational complexity compared to the S-transform. Teager energy operator increased the noise immunity. The end points and the duration of each voltage flicker component were precisely calculated through the high resolution of fast S-transform. Results showed that the relative errors were less than 5%.

In 2016, Feng Li et al. [14] proposed a method for estimating the components of voltage flicker with the help of chirp Z- transform and the Teager energy operator. The Teager energy operator having error correction factor was shown and an improved Teager energy operator was presented which decreased the errors in the voltage flicker estimation. The magnitude and frequency of voltage envelope were calculated by the Chirp Z-transform. The evaluation was done on the basis of voltage harmonics and inter-harmonics, white noise, and fluctuation of frequency. The results showed the magnitude and frequency errors of the flicker were reduced significantly. However, in the presence of input signal to noise ratio (SNR) of less than 35 dB, a reduced accuracy was found.

In 2017, Ali Dastfan et al. [15] presented a method for extraction of voltage envelope using phase-locked loop (PLL) and Grey system model (GM). Voltage envelope was detected using phase-locked loop and then the signal was uniformly sampled. Grey system theory-based models, such as GM(1,1) and the rolling Grey model were used to predict the time series. Further, the Fourier correction Grey model (FGM) was used to improve the precision of GM(1,1). Because of the lesser number of samples, an iterative approach was taken to estimate the entire voltage envelope. Results showed that Grey models were able to reduce the errors in the detection of voltage envelope by 5%.

CHAPTER 3: METHODOLOGY

3.1 THE HILBERT TRANSFORM

Leonard Euler (1707- 1783) first derived the Euler formula. Later in 1893, the scientist Charles P. Steinmetz and a physicist Arthur E. Kennelly first used this formula to form a time varying harmonic waveform in the complex form. i.e.

$$e^{j\omega t} = \cos \omega t + j \sin \omega t \qquad (3.1)$$

Later, a German scientist David Hilbert proved that the ± π/2 phase-shift of the signal is, in fact, a transform of the real part of the signal. This transform is called the Hilbert transform. He proved that $\cos \omega t$ is the Hilbert transform of $\sin \omega t$. Thus ± π/2 phase-shift is the most important property of the Hilbert transform.

3.1.1 **Hilbert Transform Definition**

Hilbert transform is an important technique in mathematics as well as in signal processing. If $x(t)$ is the real valued signal, then the Hilbert transform of this signal is $\hat{x}$(t) which can be defined as follows:

$$\hat{x}(t) = H[x(t)] = \frac{1}{\pi} \int_{-\infty}^{+\infty} \frac{x(\tau)}{t-\tau} d\tau \qquad (3.2)$$

From equation (3.2), it can be seen that time is the independent variable and it is not changed after the integration. Thus the Hilbert transform $\hat{x}$ (t) of the signal $x(t)$ is also a time dependent signal. Due to the singularity at $\tau = t$, the Hilbert transform is not calculated like the integral function, rather the above integral is considered as the Cauchy principal value of the integral function [16] having the pole at $\tau = t$.

3.1.2 **Frequency Response Of The Hilbert Transform**

The following equation shows about Hilbert transform, that it is a convolution:

$$H[x(t)] = \hat{x}(t) = \frac{1}{\pi t} * x(t) \qquad (3.3)$$

This is obtained from the convolution of $x(t)$ with 1/(πt).

As per the theorem of convolution (which states that the product of Fourier transforms of two functions is same as the Fourier transform of their convolution), the following equations show that $H[x(t)]$'s spectrum is dependent on $x(t)$.

$$F\{\hat{x}(t)\} = \frac{1}{\pi} F\left\{\frac{1}{t}\right\} F\{x(t)\} \tag{3.4}$$

Where F denotes the Fourier transform.

$$F\left\{\frac{1}{t}\right\} = \int_{-\infty}^{+\infty} \frac{1}{x} e^{-j2\pi f x} dx = -j\pi \mathrm{sgn}(f) \tag{3.5}$$

This implies that the Fourier transform of 1/ πt comes out to be − jsgn(f). So, for positive frequency, this is equal to -j and for negative frequency this is equal to +j. Thus, Hilbert transform work as a filter, where the phase of the spectral components is changed by π/2, but the amplitudes are unaltered. The phase may change negatively if the sign of the frequency is negative or positively if it is positive [17].

Thus, the Fourier transform of the f(t)'s Hilbert transform comes out to be the following:

$$F\{(\hat{x}(t))\} = -j\mathrm{sgn}(f) F\{x(t)\} \tag{3.6}$$

3.1.3 **Properties Of The Hilbert Transform**

Some of the major properties of the Hilbert transform are:

(i) Linearity: for function $f(t)$, the Hilbert transform is

$$H[f(t)] = \frac{1}{\pi} \int_{-\infty}^{\infty} \frac{f(\tau)}{t-\tau} d\tau \tag{3.7}$$

At t= τ, there is a possibility of singularity. So the above integral is considered as a Cauchy principal value [16].

$$H[f(t)] = \log_{x\to 0}\frac{1}{\pi}\int \frac{f(\tau)}{t-\tau}d\tau \qquad (3.8)$$

Suppose there is a function $f(t)$, such that

$$f(t) = c_1 f_1(t) + c_2 f_2(t)$$

Then the value of Hilbert transform of this function f(t) will be:

$$H[f(t)] = H[c_1 f_1(t) + c_2 f_2(t)]$$

$$= \log_{x\to 0}\frac{1}{\pi}\int \frac{c_1 f_1(t) + c_2 f_2(t)}{t-\tau}d\tau$$

$$= c_1 \log_{x\to 0}\frac{1}{\pi}\int \frac{f_1(t)}{t-\tau}d\tau + c_2 \log_{x\to 0}\frac{1}{\pi}\int \frac{f_2(t)}{t-\tau}d\tau$$

$$= c_1 H[f_1(t)] + c_2 H[f_2(t)] \qquad (3.9)$$

This proves that the Hilbert transform follows linearity principle.

(ii) The Hilbert transform of a Hilbert transformed function $\hat{f}(t)$ is nothing but the negative of the real signal $f(t)$:

$$H\left[\hat{f}(t)\right] = \hat{\hat{f}}(t) = F^{-1}\left[-j\mathrm{sgn}(\omega)F\left[\hat{f}(t)\right]\right]$$

$$= F^{-1}[-j\mathrm{sgn}(\omega)[-j\mathrm{sgn}(\omega)F(j\omega)]]$$

$$= F^{-1}[-F(j\omega)]$$

$$= -f(t)$$

(iii) If we take derivative of the Hilbert transform of a signal, say, $f(t)$ then it will be equal to the Hilbert transform of $f'(t)$ [18].

$$H[f(t)] = \frac{1}{\pi}\int_{-\infty}^{\infty}\frac{f(\tau)}{t-\tau}d\tau = \frac{1}{\pi}\int_{-\infty}^{\infty}\frac{f(t-s)}{s}ds$$

$$\frac{d}{dt}\{H[f(t)]\} = \frac{d}{dt}\left\{\frac{1}{\pi}\int_{-\infty}^{\infty}\frac{f(t-s)}{s}ds\right\}$$

$$= \frac{1}{\pi}\int_{-\infty}^{\infty}\frac{f'(t-s)}{s}ds$$

$$= \frac{1}{\pi}\int_{-\infty}^{\infty}\frac{f'(\tau)}{t-\tau}d\tau$$

$$= H[f'(t)]$$

(iv) The Hilbert transform of a function is orthogonal to the function

$$\int_{-\infty}^{\infty} f(t)\hat{f}(t)\,dt = \int_{-\infty}^{\infty} f(t)\left[\frac{1}{2\pi}\int_{-\infty}^{\infty} -jsgn(\omega)F(j\omega)e^{j\omega t}d\omega\right]dt$$

$$= \frac{1}{2\pi}\int_{-\infty}^{\infty} -jsgn(\omega)F(j\omega)\left[\int_{-\infty}^{\infty} f(t)e^{j\omega t}dt\right]d\omega$$

$$\frac{-j}{2\pi}\int_{-\infty}^{\infty} sgn(\omega)|F(j\omega)|^2\,d\omega$$

$$= 0$$

The integrand $sgn(\omega)|F(j\omega)|^2$ is integrated over the symmetric limits and this integrand is an odd function. Thus, the integration result comes out to be zero. This proves the property of the orthogonality. This property of Hilbert transform can find its usage in power and energy signals.

3.1.4 **Analytic Signal Using Hilbert Transform**

The Hilbert transform can also be used in the generation of the analytic signal. The analytic signal representation is a complex form of function. It can be formed by the addition of quadrature of Hilbert transform to the original signal [19]. So, the analytic signal is defined as:

$$z(t) = f(t) + j\hat{f}(t) = A(t)e^{j\theta(t)}, \quad (3.10)$$

where

$f(t)$ and $\hat{f}(t)$ is the input signal and its Hilbert transform respectively.

$z(t)$ is the analytic signal. It is also called as the pre-envelope of $f(t)$

The analytic signal $z(t)$ can be expressed in polar form as follows:

$$z(t) = A(t)e^{j\theta(t)}$$

$A(t)$ can be defined as the envelope of $z(t)$ given as follows:

$$A(t) = \sqrt{f^2(t) + \hat{f}^2(t)} \quad (3.11)$$

$\theta(t)$ can be defined as the phase of $z(t)$ given as

$$\theta(t) = \arctan\left(\frac{\hat{f}(t)}{f(t)}\right) \quad (3.12)$$

3.1.5 **Limitations Of Hilbert Transform**

(i) The singularities involved in the Hilbert transform computation is a critical subject in case of digital implementation, since Hilbert transform is computed using improper integral. In the case with discrete input data, where the required integral could not be calculated using the closed form, there are complications in the implementation of Hilbert transform.

(ii) Due to the slow decay rate and the infinite length of the impulse response of Hilbert transform, there is Gibbs phenomenon [20] in its digital implementation. Thus it reduces the precision.

3.2 **WAVELET TRANSFORM**

The meaning of the term wavelet is “small wave” [21]. These functions occur for a limited duration and their energy is concentrated around a point in time. Over the past century, wavelets have been developed and worked upon in many different fields, independently. The first system was developed by Haar in 1910, which was an alternative to the Fourier transform (developed by Fourier, in 1807) [22]. The next such system was created by Ricker [23], which models the seismic waves as they travel through the Earth. The work on wavelets increased in the 1980s with the development of continuous wavelet transform. The discrete wavelet transform and its inverse were developed in the 1990s, which allowed filtering and compression of the signals.

In Fourier transform, the signal is converted from the time domain to its corresponding frequency domain. One of the drawbacks of Fourier transform is that the signal’s information is spread across the entire range of the transform. As stated in [24], “A local characteristic of the signal becomes a global characteristic of the transform”. Gabor [25], in 1946, proposed the windowed Fourier transform. In this type of transformation, a window function of a small duration is applied to the signal and its Fourier transform is taken. This process was repeated at various different parts of the signal.

One of the limitations of Fourier transform method is that the length of the window is constant. If the feature of the signal is much shorter than the length of the window, then it becomes difficult to extract the information of the signal (since any local property within the time span of the window becomes a global property of the Fourier transform of the window, as previously stated. On the other hand, if the signal’s feature is larger than the windowing function, then its information spans over multiple windows, which again makes it difficult to extract the information. One more limitation is that the time resolution for the windowed Fourier transform for the low-frequency signals is same as to that of high-frequency signals. According to the Heisenberg’s uncertainty principle, the time resolution of the window is inversely proportional to the frequency resolution. The high-frequency signals change much faster than the low-frequency signals. Therefore, there was the requirement of such a transform by which a better time resolution can be provided to the high-frequency segments, while a better frequency resolutions can be provided to the low-frequency segments of the signal.

The wavelet transform resolves the limitations of the windowed Fourier transform by scaling the bandwidth of the filter Δf inversely to the frequency f0. According to [26], while each box of the windowed Fourier transform has the same bandwidth, each level of the wavelet transform has the same quality factor Q defined as

$$Q \equiv \Delta f / f0$$

This gives the transform the desired time resolution for the higher frequency portions and the desired frequency resolution for lower frequency portions.

3.2.1 **Principles Of Wavelet Transform**

Wavelets look like small waves in the sense that they start to grow and then decays in a fixed duration. In other words, wavelet represents a small energy signal, having finite length and amplitude. They are unlike the sinusoidal signals (used in Fourier transform) which are infinite length waves, which grow and decay in the duration of infinite time.

The fundamental idea behind wavelets is multi resolution analysis [27] or scale. The wavelet transform is a two-dimensional function, which maps the time into two parameters, scale a and translation b.The parameter 'a' performs scaling by compressing and stretching the wavelet function. Dilating (stretching) the low-frequency component of the wavelet function ψ is used for the frequency analysis while contracting (compressing) the high frequency component of the wavelet function provides temporal analysis. The parameter 'b' is the translation/shifting parameter of the wavelet function along the time axis. Wavelet analysis circumvents around the use of a wavelet function, also called the mother wavelet function, traditionally represented by the Greek letter (ψ).

For ψ to be wavelet function or mother wavelet, following are the necessary conditions.

(i) The first condition is that the wavelet function must have zero mean. In other words, it should be oscillatory, hence the word 'wavelet'. The integral over time of this function must be zero. Mathematically [28],

$$\int \psi(t)dt = 0 \qquad (3.13)$$

It ensures that wavelet has zero dc components, or in other words, any excursions the wavelet function makes above zero must be canceled out by the excursions below zero.

(ii) The second condition is that the wavelet should be of finite energy. The function should lead towards zero with time.

$$\int_{-\infty}^{+\infty} \psi^2(t) < \infty \qquad (3.14)$$

The energy of the wavelet function is usually equal to one. Sinusoidal functions such as cosine and sine do not have finite energy, hence they cannot be used as wavelet functions since they violate the second condition. This is an implicit requirement that, while the wavelet function has finite energy, it must have some energy, so the integral must be greater than zero.

(iii) The third requirement is known as the admissibility condition, which states that the Fourier transform of the wavelet function cannot have zero frequency component, i.e.

$$a_\psi = \int \frac{|\psi_f(f)|^2}{f} df \text{ satisfies } 0 < a_\emptyset < \infty \quad (3.15)$$

Where $|\psi_f(f)|$ is the Fourier transform of $\psi(t)$.

One of the wavelets satisfying above conditions is the Morlet wavelet. It is a real valued wavelet function that has a small but greater than zero value for the zero frequency value of its Fourier transform

(iv) Another condition is that the wavelet function should have effective support. While the wavelet functions for the continuous wavelet transform are usually mathematical functions that extend to infinity, effective support means that the wavelet functions are effectively zero outside a certain range.

3.2.2 Continuous Wavelet Transform

Morlet and Grossman developed the continuous wavelet transform in 1984 [29]. For the continuous wavelet transform, the wavelet function ψ is shifted in time and is scaled [28] as per the following expression:

$$\psi_{a,b}(t) = \frac{1}{\sqrt{|a|}} \psi\left(\frac{t-b}{a}\right), a, b \in R, a \neq 0 \qquad (3.16)$$

Where a= scaling parameter
b= translation/shifting parameter

The continuous wavelet transform can be expressed as the integration of function to be analyzed (here f (t)) with the complex conjugate of the wavelet function ψ^* :

$$CWT\{f(t), a, b\} = \int_{-\infty}^{\infty} f(t)\psi^*_{a,b}(t)dt \qquad (3.17)$$

3.2.3 The Morlet Wavelet Function

The performance of the continuous wavelet transform mainly lies upon the choice of wavelet functions. There are various wavelet functions for different applications, such as Gabor, Daubechies, Mexican hat, Haar, Morlet, Mallat, Coiflet. Different wavelet functions give different analysis results. The Morlet wavelet is a wavelet function used for feature extraction. It has perfect frequency domain localization. The Morlet wavelet function consists of both real and imaginary parts. This wavelet function returns information on both the amplitude and phase of the signal. It can be defined as [30]:

$$g(t) = e^{jmt}\ e^{-\frac{1}{2}(t)^2} \qquad (3.18)$$

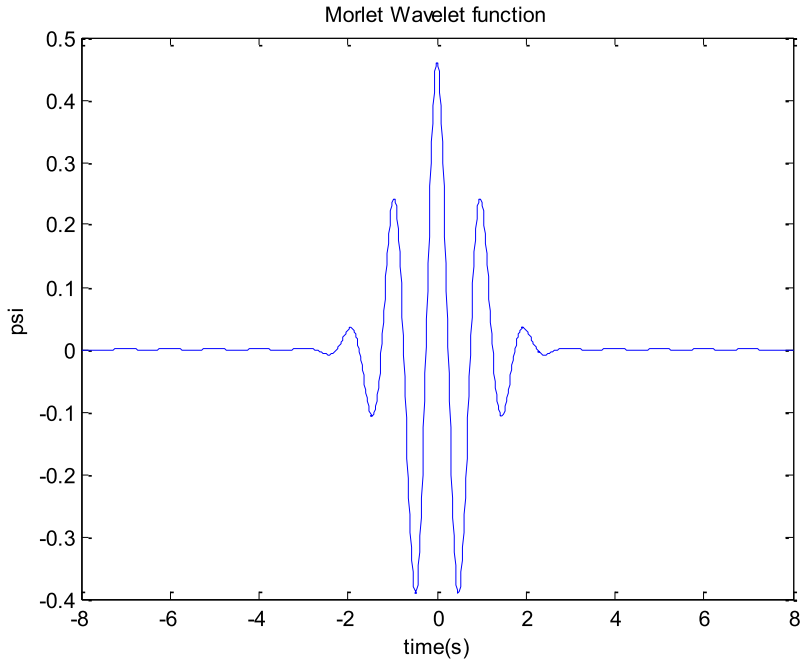

Figure1: Morlet wavelet function

In this thesis, we used the modified Morlet wavelet [31] that is:

$$g(t) = e^{jmt}\ e^{-\frac{1}{2}[(\sqrt{2}\,\sigma m/2\pi\tau)t]^2}$$

$$= \cos(mt)\, e^{-\frac{1}{2}[(\sqrt{2}\,\sigma m/2\pi\tau)t]^2} + j\sin(mt)\, e^{-\frac{1}{2}[(\sqrt{2}\,\sigma m/2\pi\tau)t]^2} \qquad (3.19)$$

m=angular frequency, τ is the number of career wave cycles; $\sigma \in R$.

3.3 WAVELET TRANSFORM AND ANALYTIC SIGNAL

In a real valued signal $L^2(R)$, (implying finite energy) the analytic signal can be calculated using the wavelet transform based method. It has been stated in [32]-[33] that with the help of continuous wavelet transform, the Gibbs phenomenon never exceeds the Gibbs phenomenon in Fourier transform; hence there are no jump discontinuities. Thus [3] proposed a method of computation of the analytic signal using wavelet transform. Because of this, the jump discontinuity that occurs, when the analytic signal is formed by the Hilbert transform, is reduced greatly and there was no Gibbs effect. The analytic signal generated using wavelet transform has better performance in terms of noise reduction as compared to the analytic signal using Hilbert transform. According to [3], if

g(t) refers to the analytic wavelet function and the Fourier transform of g(t) is $\hat{g}$(w) which satisfies the following equations:

$$g(t) \in L^1(R, dt) \cap L^2(R, dt) \tag{3.20}$$

$$\hat{g}(\omega) \in L^1(R\backslash\{0\},\ d\omega/|\omega|) \ \cap \ L^2(R\backslash\{0\},\ d\omega/|\omega|) \tag{3.21}$$

Below expression defines the wavelet transform of s(t) (the given signal) with respect to the wavelet function g(t)

$$S(b,a) = \frac{1}{a}\int_{-\infty}^{\infty} s(t)\bar{g}\left(\frac{t-b}{a}\right) dt \tag{3.22}$$

In the above expression, t and b are the part of the real-number set. It is assumed that a>0, $\bar{g}$(t) is taken as the complex conjugate of wavelet function $g(t)$. [3] Provided following two theorems:

Theorem 1: If the wavelet function $g(t)$ is analytic, $\hat{g}\ (\omega)$ is its Fourier transform and $s(t)$ is taken as a signal with finite value energy, $S(b,a)$ is the wavelet transform of $s(t)$. Then with respect to the scale ($a > 0$) and the shift b, $S(b,a)$ will be a complex function. For a constant value of a, the Hilbert transform of the original signal will be the complex function's imaginary part [34].

Theorem 2*:* If the wavelet function $g(t)$ is analytic and it has even real part $g_R(t)$ and

$$C_g = \int_0^{\infty} (\hat{g}_R(\omega)/\omega \; d\omega)$$

with $0 < C_g < \infty$.

Then for signal $s(t) \in L^2(R, dt)$,

$$\frac{1}{Cg} \int_0^{\infty} S(t,a) \; da/a = s(t) + j\, \mathrm{H}[s(t)]. \qquad (3.23)$$

Where, $S(t,a)$ is taken from equation (3.22) and $\mathrm{H}[s(t)]$ is the Hilbert transform of $s(t)$.

Proof:

$$S(t,a) = \frac{1}{a} \int_{-\infty}^{\infty} s(b) \overline{g} \left(\frac{b-t}{a}\right) db$$

$$S(t,a) = \frac{1}{a} \int_{-\infty}^{\infty} s(b) [g_R \left(\frac{b-t}{a}\right) - j g_I (\frac{b-t}{a})] db$$

$$= \frac{1}{a} \int_{-\infty}^{\infty} s(b) g_R \left(\frac{b-t}{a}\right) db \; - j \frac{1}{a} \int_{-\infty}^{\infty} s(b) g_I \left(\frac{b-t}{a}\right) db$$

$$= S_R(t,a) + j\, S_I(t,a) \qquad (3.24)$$

Where

$$g_R(t) = Re\big(g(t)\big), \qquad g_I(t) = Im(g(t))$$

$$S_R(t,a) = \frac{1}{a} \int_{-\infty}^{\infty} s(b) g_R \left(\frac{b-t}{a}\right) db \qquad (3.25)$$

$$S_I(t,a) = \frac{-1}{a} \int_{-\infty}^{\infty} s(b) g_I \left(\frac{b-t}{a}\right) db \qquad (3.26)$$

As per Theorem 1;

$$S(t,a) = S_R(t,a) + j\,S_I(t,a)$$

$$S_R(t,a) + j\,H[S_R(t,a)]$$

$$= \frac{1}{a}\int_{-\infty}^{\infty} s(b)\,g_R\left(\frac{b-t}{a}\right)db$$

$$+\ jH\left[\frac{1}{a}\int_{-\infty}^{\infty} s(b)\,g_R\left(\frac{b-t}{a}\right)db\right] \qquad (3.27)$$

If we multiply both sides of equation (3.25) by a factor of $\frac{1}{C_g a}$ and then integrating it with respect to a, we get:

$$\frac{1}{C_g}\int_0^{\infty} S_R(t,a)\,\frac{da}{a}$$

$$= \frac{1}{C_g}\int_0^{\infty}\frac{1}{a^2}\int_{-\infty}^{\infty} s(b)\,g_R\left(\frac{b-t}{a}\right)db\,da$$

$$= s(t) \qquad (3.28)$$

If we multiply both sides of equation (3.27) by a factor of $\frac{1}{C_g a}$ and then integrating it with respect to a, then equation (3.23) can be obtained.

Choice of wavelet function $g(t)$:

(i) Morlet wavelet function:

$$g(t) = e^{jmt}e^{-\frac{t^2}{2}} \qquad (3.29)$$

(ii) Modified Morlet wavelet function [31] :

$$g(t) = e^{jmt}\ e^{-\frac{1}{2}[(\sqrt{2}\,\sigma m/2\pi\tau)t]^2} \qquad (3.30)$$

Let C=($\sqrt{2}\,\sigma m/2\pi\tau$). In the above equation 'm' represents angular frequency, the number of carrier wave cycles is represented by the symbol 'τ', 'σ' signifies the real number related to precision. From the point of view of numerical calculation, in the case where $m^2 = (4C^2)$ is large enough then the wavelet defined in the equation (3.30) satisfies Theorem 2. Equation (3.30) wavelet function is taken as the reference for all the examples in this thesis.

Compact support is not provided to the wavelets in (3.29) and (3.30) but the decay rate of their amplitude is $e^{-\frac{t^2}{2}}$ and $e^{-\frac{1}{2}[(\sqrt{2}\,\sigma m/2\pi\tau)t]^2}$ when it is away from its center, hence the wavelet transform can provide better and accurate results compared to the Hilbert transform. The decay rate of the filter factor of Hilbert transform is 1/t.

Definition of Instantaneous Parameters

Instantaneous parameters are defined as:

1. $e(t) = \sqrt{s^2(t) + H^2[s(t)]}$
2. $\theta(t) = arctan\left(\frac{H[s(t)]}{s(t)}\right)$
3. $f(t) = \frac{1}{2\pi}\frac{d}{dt}\left[arctan\left(\frac{H[s(t)]}{s(t)}\right)\right]$

Where $e(t)$ is the instantaneous amplitude, $\theta(t)$ is the instantaneous phase angle, $f(t)$ is the instantaneous frequency of the signal $s(t)$. H denotes the Hilbert transform.

3.4 AM- FM DECOMPOSITION

The transfer of information in many naturally occurring phenomenon and also in many artificial systems is done by varying the amplitude and frequency of the signal. Some of those systems consist of both time varying amplitude and frequency, simultaneously. Such systems can be called as amplitude modulation- frequency modulation (AM/FM) models. The decomposition of such signals into the amplitude and frequency modulated sinusoids are useful in many applications including speech processing and music analysis, such as audio coding, audio transformation, speech recognition etc. The representation of the AM-FM model is also desirable in various audio effects, for example, scaling of time, pitch-shifting.

It has been stated by K. Saberi [35] and R. McEachern [36] that our ear cannot identify the signal waveforms; that is human ear cannot detect the change in amplitude and frequency directly. That is why no transformation theory is possible in case of human's ear. Also, the information contained in the envelope of the speech signals dominates as that of the fine structure (i.e FM) [37]. While in the case of melodies, the importance of the fine structure is high. Hence in the application of speech analysis, it is important to decompose a signal into its corresponding AM-FM components. Therefore this decomposition is very useful in speech and music signal processing [38,39].
In general, the AM/FM signal is represented by real part of the complex signal $[A(t), \phi(t)]$ and can be modeled as follows:

$$x(t) = A(t)\cos[\emptyset(t)] = Re[A(t)e^{j\phi(t)}] \quad (3.31)$$

Where instantaneous amplitude of the signal $x(t)$ is $A(t)$. This is also called as envelope of the signal. $\phi(t)$ is the instantaneous phase angle. The FM is the derivative of the phase $\phi(t)$ i.e the instantaneous frequency of the signal. Finding a pair of AM-FM signal that solves equation (3.31) is the main purpose of AM-FM decomposition. This decomposition results in infinitely many combinations as this decomposition is not unique. There could be many pairs that satisfy the above equation. This issue is addressed in [40]. Such a pair could be calculated by combining signal $x(t)$ with its analytic signal. With the help of analytic signal, the corresponding AM and FM can be found. Thus, we can say that the decomposition problem is finding AM and FM pair that satisfies (3.31) with a condition that $A(t)e^{j\phi(t)}$ is the analytic signal.

Let $z(t)$ be an analytic signal, and $\tilde{x}(t)$ is the Hilbert transform of the signal $x(t)$. Then,

$$z(t) = x(t) + j\tilde{x}(t). \quad (3.32)$$

Then,

$$A(t) = |z(t)| = \sqrt{x^2(t) + \tilde{x}^2}(t)$$
$$\phi(t) = \arg[z(t)] = \tan^{-1}\frac{\tilde{x}(t)}{x(t)}$$
$$\omega(t) = \phi'(t) \quad (3.33)$$

For example, consider AM-FM signal

$$x(t) = (1 + 0.5cos\omega_1(t))cos\omega_2(t) \quad (3.34)$$

Or,

$$x(t) = \mathrm{Re}(\left(1 + 0.5cos\omega_1(t)\right)e^{j\omega_2 t})$$

$$\tilde{x}(t) = \left(1 + 0.5cos\omega_1(t)\right)\sin\omega_2(t)$$

Or,

$$\tilde{x}(t) = \mathrm{Img}(\left(1 + 0.5cos\omega_1(t)\right)e^{j\omega_2 t})$$

The corresponding analytic signal is:

$$z(t) = (1 + 0.5cos\omega_1(t))e^{j\omega_2 t}$$

$$A(t) = |1 + 0.5cos\omega_1(t)| = (1 + 0.5cos\omega_1(t))$$

$$\phi(t) = \tan^{-1}(\sin\omega_2(t)/\cos\omega_2(t)) = \omega_2 t$$

$$\omega(t) = \omega_2$$

The corresponding AM, PM, FM of the spatial signal $x(t)$ is shown in Figure 2. The values taken are $\omega_1 = 5\pi, \omega_2 = 20\pi$ radians per second respectively.

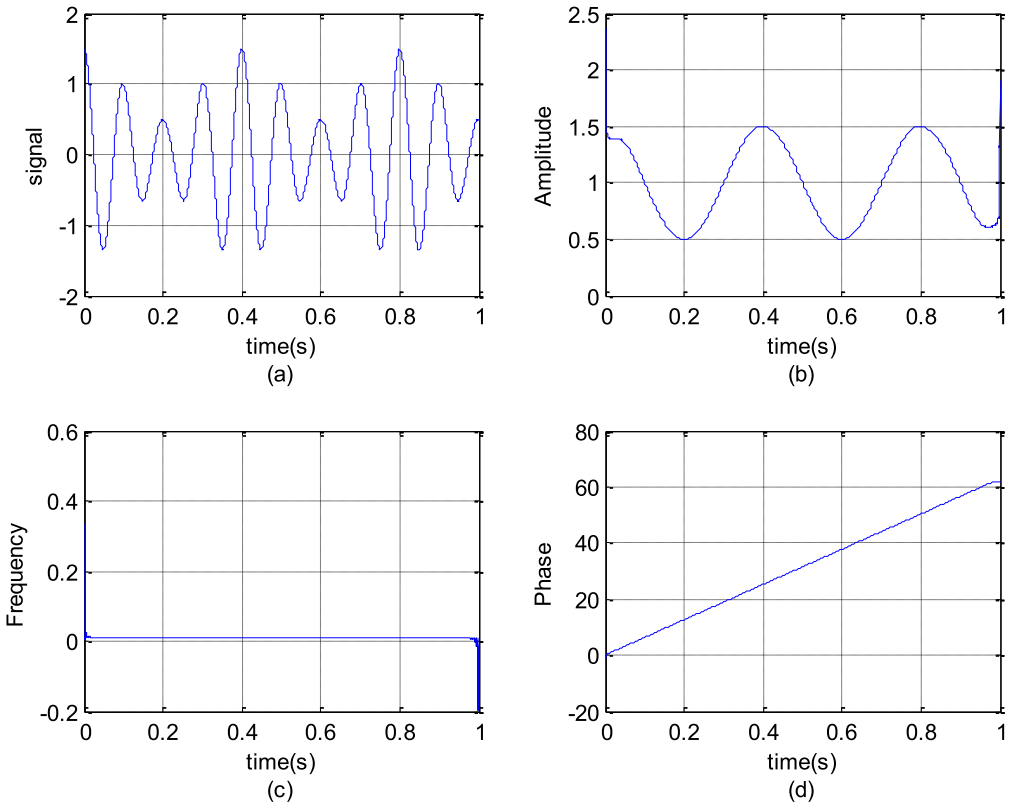

Figure 2: AM-FM model and its corresponding parameters (a) signal, (b) AM, (c) FM, and (d) PM.

3.4.1 Over-Modulated AM-FM Signal

The estimation of the frequency modulation (FM) and amplitude modulation (AM) of a real valued signal could be a difficult drawback when AM has zero crossings. Most of the cases assume that the amplitude modulation or the envelope of the signal cannot go negative. This assumption is not correct. In many cases, the envelope of the speech and music signal takes negative values. Such cases come under over-modulation. While, the envelope that has only the positive values of amplitude comes under the category of under-modulation. In the case of over-modulation, if the measured signal is crossing zero value but the corresponding amplitude modulation or instantaneous amplitude is detected positive, then the phase of the signal inhibits a phase jump of the value π. This phase jump results in discontinuities in the FM. Therefore, the reconstructed signal will be full of distortions. Over-modulation is a natural phenomenon and can be seen not only in man-made signals but also in naturally occurring events such as speech and music.
According to L. Cohen, P. Loughlin [41], equation (3.33) defines the AM, PM, and FM for the signals having modulation index for the amplitude modulation less than one. The modulation index of amplitude modulation can be expressed as:

$$\text{Modulation Index} = \frac{\max(AM) - \min(AM)}{\max(AM) + \min(AM)}$$

Again, if $z(t) = A(t)e^{j\emptyset(t)}$ and $A(t)$ has zero- crossings,
Then using (3.33) we get

$$A_c(t) = |A(t)| \; and \; \emptyset_c(t) = \emptyset(t) + \pi u\big(-A(t)\big), \qquad (3.34)$$

Here c accounts for the fact that they are generated by using the definitions of equation (3.33). Here the unit step function is denoted by u and it takes in account the effects of negative excursions of $A(t)$. In PM, $\emptyset_c(t)$ we get π-step discontinuities due to sign changes in $A(t)$. This phase discontinuity generates delta Dirac pulses in the corresponding FM, which is the derivative of the PM. The derivative of step function results in impulses at instants where the change in step takes place. In order to get AM, PM and FM free from distortions different techniques have to be considered.

3.5 PRONY ANALYSIS

This method was first developed by Gaspard Riche de Prony in the year 1795. It is widely popular in power system transient studies [42], [43]. Like the Fourier transform, Prony analysis takes out important information from the uniformly sampled signal. Then, series of sinusoids or damped complex exponentials are formed [44]. In other words, Prony analysis is a technique for linear estimation that fits a sum of exponentially damped complex sinusoids to samples that are uniformly spaced. With the help of those estimated sinusoids, parameters such as amplitude (A), damping factor (σ), phase (ϕ) and frequency (f) is calculated from the given signal. Below is the brief outline of the method:

Consider a continuous noiseless signal y(t), containing n number of oscillatory modes, then y(t) can be represented as:

$$\hat{y}(t) = \sum_{i=1}^{n} A_i e^{\sigma_i t} \cos(2\pi f_i t + \emptyset_i) \qquad for\ t \geq 0 \qquad (3.35)$$

Where

$\mathrm{A_i} = \text{Amplitude}$
$\sigma_\mathrm{i} = \text{damping factor}$
$\emptyset_\mathrm{i} = \text{phase}$
$\mathrm{f_i} = \text{frequency}$

By rearranging the above equation and using Euler's formula, $\hat{y}$(t) can be written as:

$$\hat{y}(t) = \sum_{i=1}^{m} R_i e^{\lambda_i t} \qquad (3.36)$$

Where

$\mathrm{R_i}$ is the complex amplitude of the i^{th}pole.

The system order m is twice of n because; each oscillatory mode is represented by one complex conjugate eigenvalue pair.

Now, assuming that $\hat{y}$(t) contains N samples uniformly spaced by a value equal to Δt, then, equation (3.36) in the discrete-time form can be written as:

$$\hat{y}(k) = \sum_{i=1}^{m} R_i z_i^k \ , for\ k = 0,1, \dots N-1 \qquad (3.37)$$

Where $z_i^k = e^{\lambda_i \Delta t}$ is the discrete-time pole

The aim of this method is to estimate R and z to the best approximate of the actual observed signal in the least square sense, i.e.

$$\hat{y}(k) = y(k) \text{ , for all values of k.} \qquad (3.38)$$

In general, Prony analysis is the set of linear equations to find out roots of a polynomial. Steps taken in the process is discussed below:

1) The first step is the collection of the measured data and construction of a linear prediction matrix. With the help of this matrix, autoregressive coefficients are calculated.

2) A polynomial equation is then formed by step (1). Next step is the calculation of the roots of the polynomial.

3) Third step is the estimation of the amplitude R and z (sinusoidal phase) by solving equation (3.38) using least mean square method.

Assuming that the current values can be approximated as a sum of weighted past values, then the linear prediction model based on equation (3.37) is defined as:

$$y[k] = a_1 y[k-1] + a_2 y[k-2] + \cdots .. + a_m y[k-m] \qquad (3.39)$$

Where, the symbol a represents the autoregressive coefficients.
These parameters are determined by solving a set of linear equations:

$$\begin{aligned} y[k] &= a_1 y[k-1] + a_2 y[k-2] + \cdots .. + a_m y[k-m] \\ y[k+1] &= a_1 y[k] + a_2 y[k-1] + \cdots .. + a_m y[k-m+1] \\ y[k+2] &= a_1 y[k+1] + a_2 y[k] + \cdots .. + a_m y[k-m+2] \\ y[N] &= a_1 y[N-2] + a_2 y[N-3] + \cdots .. + a_m y[N-m-1] \end{aligned} \qquad (3.40)$$

Alternatively, equation (3.40) can be expressed in matrix form

$$\begin{bmatrix} y(m) \\ y(m+1) \\ \vdots \\ y(N-1) \end{bmatrix} = \begin{bmatrix} y(m-1) & y(m-2) & \cdots & y(0) \\ y(m) & y(m-1) & \cdots & y(1) \\ \vdots & \vdots & \cdots & \vdots \\ y(N-2) & y(N-3) & \cdots & y(N-m-1) \end{bmatrix} \begin{bmatrix} a_1 \\ a_2 \\ \vdots \\ a_m \end{bmatrix} \qquad (3.41)$$

Note: In the digital implementation, it has been seen that in most cases the total samples N are not equal to twice of m, but they are greater than twice of m. Such a matrix is called over-determined matrix. Hence, in this case, the autoregressive coefficients are determined using the pseudo-inverse matrix. The appropriateness of the constructed data matrix depends on the following factors:

1) The spread of the measured input, and

2) The number of available samples. Since the monitoring window is usually predefined and fixed, care is needed for selecting the sampling interval.

Once the coefficients a are found, the roots of the polynomial (equation 3.42) are calculated. These roots are also the eigen values.

$$z^m - (a_1 z^{m-1} + a_2 z^{m-2} + \cdots + a_m) = 0 \tag{3.42}$$

The primary advantage of Prony analysis is that it does not require any prior knowledge of the system model to conduct its approximation. However, it is a time-invariant method, i.e. the network dynamics are assumed to be constant within the same sampling time window.

CHAPTER 4: METHOD DESCRIPTION

Overview:

This work presents detection of instantaneous flicker level by extracting the frequency, phase angle, and magnitude of the voltage inter-harmonic component using Prony analysis [1] and computation of frequency, amplitude and phase modulations using the vector interpretation of the analytic signal [2]. These two applications of the analytic signal have been done by computing the instantaneous parameters (instantaneous amplitude, instantaneous frequency, and Instantaneous phase) using the wavelet transform based method and compared with Hilbert transform based method.

4.1 ESTIMATION OF AMPLITUDE, FREQUENCY AND PHASE MODULATIONS

This section presents the computation of AM, FM, and PM when the signal has zero crossings, or when AM is over-modulated. It has been done using analytic signal. This is a two step process. (i) The analytic signal is generated, and (ii) The square of analytic signal is used for finding the AM, PM and thus FM of the over-modulated sinusoidal model [2]. In this, the analytic signal is interpreted as a vector function. Then a unit vector is considered, where the square of the dot product of analytic signal and the unit vector is maximized at each instant. This results in the computation of eigen values. The PM is defined by taking the orientation of the most optimum eigenvector. Block diagram of the above method is shown in Figure 3. In this way, we can get zero crossing AM and distortion-less PM. We then use a direct equivalence of eigen value problem to the squared analytic signal which is computationally simple [2] as shown in Figure 4.

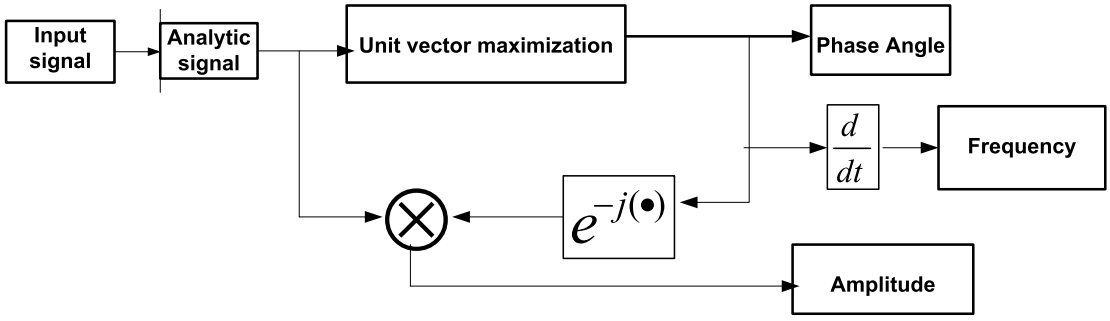

Figure 3 Block diagram for AM-FM decomposition

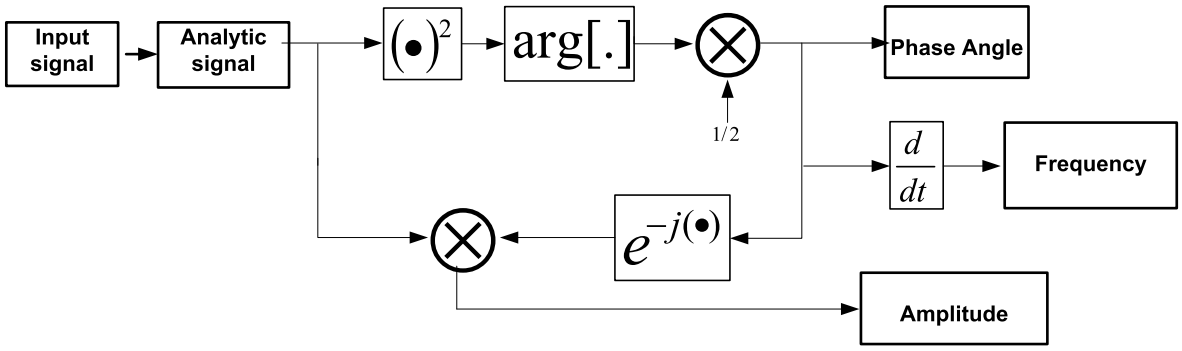

Figure 4: Block diagram of AM-FM decomposition using squared analytic signal

4.1.1 Computation Of Phase and Amplitude Functions

Fractional Hilbert transform [45] can be used to make a generalization of the phase angle of the Hilbert transform. It is used to make phase angle from $\frac{\pi}{2}$ to angle $\emptyset$. Here $\emptyset$ belongs between $-\pi \ to + \pi$. Let $\tilde{x}_{\emptyset}(t)$ specifies fractional Hilbert transform of x(t) . Then, we have that

$$\tilde{x}_{\emptyset}(t) = \mathcal{H}_{\emptyset}\{x\}(t) \triangleq x(t)\cos\emptyset + \tilde{x}(t)\sin\emptyset \quad (4.1)$$

4.1.1.1 Phase modulation

Since the analytic signal $x_a(t)$ of signal $x(t)$ is given as:

$$x_a(t) = x(t) + j\tilde{x}(t) .$$

The real part $x(t)$ and imaginary part $\tilde{x}(t)$ of the analytic signal has phase difference of 90^o. Therefore we can say that they are mutually orthogonal to each other, i.e.

$$\langle x(t), \tilde{x}(t)\rangle = 0$$

We can represent the analytic signal vector by $x_a(t) = [x(t)\tilde{x}(t)]^T$
Next, considering a unit vector $u_{\emptyset}$ with orientation angle $\emptyset$ such that

$$u_{\emptyset} = [cos\emptyset \ sin\emptyset\ ],^T .$$

The inner-product of $u_{\emptyset}$ with $x_a(t)$ is:

$$r(t) = u_{\emptyset}^{T} x_a(t) = x(t)\cos\emptyset + \tilde{x}(t)\sin\emptyset \qquad (4.2)$$

Now we maximize $r^2(t)$ with respect to the angle $\emptyset$, to find angle $\dot{\emptyset}(t)$ such that

$$\dot{\emptyset}(t) = \arg\max r^2(t) = \arg\max |\mathcal{H}_{\emptyset}\{x\}(t)|^2$$

$$= \arg\max u_{\emptyset}^{T} J\big(x(t)\big) u_{\emptyset} \qquad (4.3)$$

Where $J\big(x(t)\big) = \begin{bmatrix} x^2(t) & x(t)\tilde{x}(t) \\ x(t)\tilde{x}(t) & \tilde{x}^2(t) \end{bmatrix}$ is the Jacobian matrix of $x(t)$ such that the coloums of the matrix denotes eigen vectors corresponding to each eigen value.

Equation (4.3) shows that that the eigen vector with largest eigenvalue of $J(x(t))$ is the direction of optimal $u_{\emptyset}$. This is similar to the matched filter operation where a unit vector is used as a template at every instant. We then find direction of that unit vector that gives maximum value of correlation with the analytic signal vector. The maximization in equation (4.3) yields two solutions:

$$\dot{\emptyset}_1(t) = \frac{1}{2}\tan^{-1}\left(\frac{2x(t)\tilde{x}(t)}{x^2(t) - \tilde{x}^2(t)}\right)$$

$$\dot{\emptyset}_2(t) = \dot{\emptyset}_1(t) + \pi \qquad (4.4)$$

$\dot{\emptyset}_1$ and $\dot{\emptyset}_2$ are 180 degrees apart from each other. Since the determinant of the matrix $J(x(t))$ is zero, the matrix $J(x(t))$ is singular.
The eigen values of the matrix $J(x(t))$ are calculated as zero and $x^2(t) + \tilde{x}^2(t)$.
Where, $x^2(t) + \tilde{x}^2(t)$ is magnitude square of analytic signal $x_a(t)$. This is also the definition of the energy of a signal. In this case the energy signal is the analytic signal.
Both of the columns of the matrix $J(x(t))$ have the following relation:

$$\begin{bmatrix} x(t)\tilde{x}(t) \\ x^2(t) \end{bmatrix} = c^t \times \begin{bmatrix} x^2(t) \\ x(t)\tilde{x}(t) \end{bmatrix}$$

In the above equation, $c^t = \frac{\tilde{x}(t)}{x(t)} = tan\theta(t)$ is the tangent of phase modulation calculated using conventional definition (equation 3.33). We show $\dot{\emptyset}(t)$= $\dot{\emptyset}_2(t)$ as new definition of

PM of $x_a(t)$. This definition forms the PM which is free from discontinuities. We can construct new AM $\dot{A}(t)$ such that

$$\dot{A}(t) = x_a(t)\, e^{-j\,\dot{\phi}(t)}$$

$$= \cos\dot{\phi}(t)\big(x(t) + \tilde{x}(t)\tan\dot{\phi}(t)\big) + \mathrm{j}\cos\dot{\phi}(t)\big(\tilde{x}(t) - x(t)\tan\dot{\phi}(t)\big)$$

Since $\tan\dot{\phi}(t) = \frac{\tilde{x}(t)}{x(t)}$

$$\dot{A}(t) = \frac{x^2(t) + \tilde{x}^2(t)}{x(t)}\cos\left(\frac{1}{2}\tan^{-1}\left(\frac{2x(t)\tilde{x}(t)}{x^2(t) - \tilde{x}^2(t)}\right)\right) \qquad (4.5)$$

Equation (4.4) is considered as new definition of phase modulation (PM) of $x_a(t)$ and equation (4.5) is the new amplitude modulation for $x_a(t)$. Further, the frequency modulation (FM) is then calculated by taking differentiation of PM. The analytic signal constructed using new definitions $\dot{A}(t)$ and $\theta(t)$ is given as:

$$x_a(t) = A(t)e^{j\theta(t)}.$$

Then, solving (4.3) we get

$$\dot{\phi}(t) = \frac{1}{2}\tan^{-1}\frac{2A^2(t)\sin\theta(t)\cos\theta(t)}{A^2(t)\big(cos^2\,\theta(t) - sin^2\,\theta(t)\big)} = \theta(t) \qquad (4.6)$$

Since, in equation (4.6), the term $A^2(t)$ is always positive, therefore the sign of this term or the amplitude of the signal doesn't make any effect on $\dot{\phi}(t)$. Consequently, there would not be any jump discontinuities due to the zero crossings of $A(t)$. And thus, we can conclude that the phase modulation is free from π −step phase jumps. Hence, differentiation of the phase angle, which is in fact the frequency modulation, does not contain the delta Dirac impulses. Also, the new phase modulation and the conventional phase modulation (equation 3.33) can be related as:

$$\dot{\phi}(t) = \theta_c - \pi u\big(-A(t)\big) \qquad (4.7)$$

4.1.1.2 Computation of phase and amplitude functions by squaring the analytic signal

$x_a(t)$ can be expressed in polar form as $x_a(t) = \sqrt{x^2(t) + \tilde{x}^2(t)}\ e^{jtan^{-1}\left(\frac{\tilde{x}(t)}{x(t)}\right)}$. Let $y_a(t)$ be the square of the signal, such that, $y_a(t) = x_a^2\ (t)$, then:

$$y_a(t) = \ (x^2(t) + \tilde{x}^2(t))\ e^{j2tan^{-1}\left(\frac{\tilde{x}(t)}{x(t)}\right)}$$

$$|y_a(t)| = \ (x^2(t) + \tilde{x}^2(t)),\ \text{and}$$

$$\arg[\ y_a(t)] = 2\tan^{-1}\left(\frac{\tilde{x}(t)}{x(t)}\right)$$

$$= \ \tan^{-1}\left(\frac{2x(t)\tilde{x}(t)}{(x^2(t)-\tilde{x}^2(t)}\right) \qquad (4.8)$$

On comparing equations (4.4) and (4.8), it is observed that $\arg[\ y_a(t)] = 2\dot{\emptyset}(t)$.
Basically, the angle given by the eigenvector formalism, corresponding to the square of analytic signal is up to a scale factor of 2. The square of analytic signal can also explain the smooth nature of $\dot{\emptyset}(t)$. The reversal of polarity in $A(t)$ causes the π -step jumps in the conventional PM $tan^{-1}\ (\frac{\tilde{x}(t)}{x(t)})$. Squaring of the analytic signal converts the π–step jumps to 2π–step jumps. The smooth phase is the result of their absorption by the exponential $e^{j(.)}$, that is:

$$y_a(t) = \ |A(t)|^2 e^{j(2\theta(t)+\ 2\pi u(-A(t)))} = \ A^2(t)e^{j2\theta(t)}$$

$$|y_a(t)| = \ A^2(t),\ \text{and}$$

$$\arg[y_a(t)] = 2\theta(t) = 2\dot{\emptyset}(t) \qquad (4.9)$$

The above equations give new definition of the phase modulation which can be obtained using the squared form of the analytic signal [2]. The phase angle calculated by squaring

the analytic signal is twice that of the phase angle obtained using the eigen vector method of phase calculation. Since the method of squaring the analytic signal is simple compared to that of equation (4.3), so in this thesis, we used the squared analytic signal for the analysis.

4.2 ESTIMATION OF VOLTAGE ENVELOPE

The voltage fluctuation analysis is an important parameter to analyze the power quality in the power systems. Thus, the detection of voltage fluctuation is desirable in many industrial applications. These fluctuations are the variations in the amplitude of the voltage also called as voltage envelope (VE) and the variations in the fundamental frequency of the voltage. In general, it occurs at frequency variation in the range less than 30Hz. These variations in the frequency and amplitude of voltage waveform give rise to disturbances in the light sources, also termed as light flicker. Some examples where these flickers occur are electric arc furnaces, large motors, industrial loads, variable frequency drives, roll steel furnace etc. These flickers result from magnitude and frequency of the voltage envelope. Hence the voltage envelope is also called as instantaneous flicker level (IFL). The instantaneous flicker level may consist of single frequency as well as a band of frequencies.

This discussion represents the digital implementation of instantaneous flicker level detection using combined Prony decomposition method [1] and analytic signal using wavelet transform. It has been shown that the extraction of fundamental frequency components such as amplitude, phase, and frequency of voltage flickers are approximated using Prony analysis [1], while analytic signal can be applied to the predicted signal to calculate the envelope of the voltage flicker signal.

4.2.1 The Voltage Waveform

The waveform of the voltage fluctuation can be represented as amplitude modulated signal, where the amplitude of the voltage signal is varied according to the amplitude, frequency and phase of inter-harmonic components. In other words, this is a signal where the carrier wave of the power signal is modulated by amplitude and frequency of fluctuations. This waveform can be represented as:

$$v(t) = \left[A_\circ + \sum_{i=1}^{m} A_i \cos\left(\omega_{fi} t + \emptyset_{fi}\right)\right] \cos(\omega_\circ t + \emptyset_\circ)$$

$$= A_{\circ}\cos(\omega_{\circ}t + \emptyset_{\circ}) + \sum_{i=1}^{m} A_i' \cos(\omega_{IH}^{-}t + \emptyset_{IH}^{-})$$

$$+ \sum_{i=1}^{m} A_i' \cos(\omega_{IH}^{+}t + \emptyset_{IH}^{+}) \qquad (4.10)$$

Where amplitude, frequency, and phase of fundamental frequency component are $A_{\circ}, \omega_{\circ}, \emptyset_{\circ}$, and that of inter harmonic components are $A_i, \omega_{fi}, A_i', \emptyset_{fi}, \omega_{IH}^{-}, \emptyset_{IH}^{-}, \omega_{IH}^{+}, \emptyset_{IH}^{+}$ respectively.

4.2.2 Prony Analysis Decomposition Technique

Prony analysis is a method by which a complex exponential signal can be expressed as a linear summation of uniformly sampled signals. With the use of the least square method, it provides the best possible fit of the measured (input) signal. For example, if we assume that there are N samples of the signal $x(t)$, and the discretised version of the signal $x(k\Delta t) = x(k)$ where k= 0,1,2,3,….N-1, then $x(k)$ can be modeled as a linear mixture of n+1 different modes such that:

$$\hat{x}(k) = \sum_{i=0}^{n} A_i e^{(\alpha_i + j\omega_i)k\Delta t + j\emptyset_i} = \sum_{i=0}^{n} B_i z_i^k \qquad (4.11)$$

$$\text{here } B_i = A_i e^{j\emptyset_i}$$

$$z_i = e^{(\alpha_i + j\omega_i)\Delta t} = e^{\lambda_i \Delta t}$$

Where A_i, α_i, ω_i represents amplitude, damping factor, and frequency (radians per second) respectively. Also, Δt is the sampling time, $\emptyset_i$ is the initial angle of phase.

The amplitude B_i and the eigenvalue λ_i can be approximated using the least square error technique over the squared error on N samples of the signal x(k). Mathematically, this can be represented as:

$$E = \sum_{k=0}^{N-1} {e_k}^2 = \sum_{k=0}^{N-1} (x_k - \hat{x}_k)^2 \qquad (4.12)$$

The Prony method can be applied to solve equation (4.12) as follows.

Step 1) Construction of linear prediction model (LPM)

$$\begin{bmatrix} \hat{x}(n) \\ \hat{x}(n+1) \\ \vdots \\ \hat{x}(N-1) \end{bmatrix} = \begin{bmatrix} x(n-1) & x(n-2) & \cdots & x(0) \\ x(n) & x(n-1) & \cdots & x(1) \\ \vdots & \vdots & \cdots & \vdots \\ x(N-2) & x(N-3) & \cdots & x(N-n-1) \end{bmatrix} \times \begin{bmatrix} a_1 \\ a_2 \\ \vdots \\ a_n \end{bmatrix} \quad (4.13)$$

Or $\mathbf{X} = \emptyset\mathbf{A}$

Where **A** is obtained using the pseudoinverse of matrix ∅**;**

$$\mathbf{A} = \emptyset^{\dagger}\mathbf{X} = (\emptyset^{\mathbf{T}}\emptyset)^{-\mathbf{1}}\emptyset^{\mathbf{T}}\mathbf{X}$$

Step 2) Roots or eigen values of the characteristic polynomial can be obtained from step (1) as:

$$z^n - a_1 z^{n-1} - a_2 z^{n-2} - \cdots - a_n = 0 \quad (4.14)$$

Where $\lambda_i = \log\left(\frac{z_i}{\Delta t}\right) = \alpha_i \pm j\omega_i$

The eigen values λ_i gives the damping factor α_i and the angular frequency ω_i of the inter-harmonics.

Step 3) The phase angle and the amplitude can be calculated considering equation (4.11). With the result obtained in step (2);

$$\begin{bmatrix} \hat{x}(0) \\ \hat{x}(1) \\ \vdots \\ \hat{x}(N-1) \end{bmatrix} = \begin{bmatrix} z_1^0 & z_2^0 & \cdots & z_n^0 \\ z_1^1 & z_2^1 & \cdots & z_n^1 \\ \vdots & \vdots & \cdots & \vdots \\ z_1^{N-1} & z_2^{N-1} & \cdots & z_n^{N-1} \end{bmatrix} \times \begin{bmatrix} B_1 \\ B_2 \\ \vdots \\ B_n \end{bmatrix} \quad (4.15)$$

Or $\mathbf{X} = \Lambda\mathbf{B}$

Where **B** can be obtained by the pseudoinverse of matrix Λ**;**

Thus, the signal $\hat{x}(k)$ can be represented as

$$\hat{x}(k) = \sum_{i=0}^{n} A_i' \cos(\omega_i k\Delta t + \emptyset_i) \qquad (4.16)$$

For more precise calculation of linear prediction model as obtained in equation (4.15) to be the measured signal x(k), number of samples, N, quantity of distinct modes n, and the dimension of the window is varied until the linear prediction model becomes optimally closer to the simulated signal x(k).

4.2.3 Voltage Envelope Detection Using Analytic Signal

The voltage envelope can be determined using wavelet transform [3] and compared the same by calculating instantaneous parameters using Hilbert transform.

For a real valued signal, $y(t) = \cos \omega t$ the corresponding Hilbert transform part is $y_H(t) = \sin \omega t$ and the analytic signal (AS) can be expressed by the following equation:

$$x(t) = y(t) + j\, y_H(t) \qquad (4.17)$$

Therefore, the analytic signal of the estimated signal $\hat{x}(k)$ can be expressed as

$$y(k) = \hat{x}(k) + j\, \hat{x}_H(k)$$

And the envelope is

$$|y(k)| = \sqrt{(\hat{x}^2(k) + \hat{x}_H^2(k))} \qquad (4.18)$$

Or

$$y(k) = \sqrt{\left[\sum_{i=0}^{n} A_i' \cos(\omega_i k\Delta t + \emptyset_i)\right]^2 + \left[\sum_{i=0}^{n} A_i' \sin(\omega_i k\Delta t + \emptyset_i)\right]^2}$$

CHAPTER 5: SIMULATION RESULTS AND DISCUSSION

This chapter presents the simulation of

(i) Voltage envelope detection using Prony analysis and analytic signal
(ii) Computation of amplitude, phase and frequency modulation using vector interpretation of analytic signal

We simulate the above mentioned two applications of the analytic signal by calculating the instantaneous parameters using wavelet transform based method [3] and then compare the results by calculating the instantaneous parameters using the Hilbert transform method [1], [2].

5.1 Estimation of Voltage Envelope via Prony Decomposition and Analytic Signal.

This section presents the simulation of detection of voltage fluctuation level or the envelope of the voltage flicker signal and estimation of frequency, phase, and amplitude of all the frequency components of voltage envelope. We used MATLAB 7.10.0(R2010a) for this purpose. Prony's method has been implemented to extract the amplitude, frequency, phase of the voltage envelope. Then, the wavelet transform based method has been applied to obtain the analytic signal. The envelope of the fundamental frequency component has also been predicted using the analytic signal.

5.1.1 Simulation

We implemented the voltage envelope detection on two different simulated voltage signals. They are:

Case (1): Simulation of an amplitude modulated signal with single low-frequency band given as:

$$v(t) = [1 + 0.2\cos(0.2\omega_o t)]\cos(\omega_o t) \; + \; w(t) \qquad (5.1)$$

Case (2): Simulation of voltage fluctuation formed by a wide band of frequency (load current) given as:

$$i(t) = \sin(\omega_o t)\,[1 + r\sin(\omega_m t) + \; r^2\sin^2(\omega_m t) + r^3\sin^3(\omega_m t) + \cdots] \; + w(t) \quad (5.2)$$

Both of the above signals are sampled at a sampling time $T_s = 0.001$ s over a frequency of f_o= 60 Hz (fundamental frequency) i.e. ($\omega_o = 2\pi f$). The total number of samples are N=250. In case (2), we used $r = 0.5$ and $f_m = \; 8$ Hz. $w(t)$ is the additive white Gaussian noise (AWGN) of 20 dB SNR.

5.1.2 **Prony Analysis**

To implement the Prony analysis on the above examples we used the following data:

For case (1), the number of modes used in Prony analysis are n=6. Using Prony analysis, the signal of equation (5.1) is decomposed into its various frequency components shown in Table I. It shows that the fundamental component alters at a beat frequency of 12 Hz.

For case (2), the number of modes used in Prony analysis are n=125. The Prony's analysis for signal of equation (5.2) is shown in Table II. It shows that the input waveform consists of 36, 44, 52, 60, 68, 76, 84- Hz inter-harmonics causing the light flicker.

Frequency Component	Frequency Hz	Amplitude pu	Phase Angle Degree
1	72.00	0.10	+0.00
2	48.00	0.10	+0.00
3	60.00	1.00	-0.00

Table 1: ESTIMATION USING PRONY ANALYSIS FOR CASE 1 (SINGLE LFB VOLTAGE SIGNAL)

Frequency Component	Frequency Hz	Amplitude pu	Phase Angle Degree
1	36.00	0.0222	+180.00
2	44.00	0.0829	+90.00
3	52.00	0.3094	+0.00
4	60.00	1.1547	-90.00
5	68.00	0.3094	-180.00
6	76.00	0.0829	+90.00
7	84.00	0.0222	-0.00

Table II: ESTIMATION USING PRONY ANALYSIS FOR CASE 2 (WFB CURRENT SIGNAL)

5.1.3 Envelope Detection

The envelope of fundamental frequency component can be calculated using analytic signal. The envelope of a signal is calculated by taking the absolute value of its corresponding analytic signal. We used wavelet transform based analytic signal to calculate the instantaneous parameter for voltage flicker envelope detection and compared the voltage flicker envelope detection using instantaneous parameter using Hilbert transform method.

The envelope of the reconstructed signal is calculated using wavelet transform [3]. Equation (3.22) and (3.23) are used for this purpose. The wavelet function used is given as:

$$g(t) = e^{jmt} \; e^{-\frac{1}{2}[(\sqrt{2}\,\sigma m/2\pi\tau)t]^2}$$

The parameters used are m=28.28, $\sigma = 5$, $\tau = 4$, a=32, b=41

The envelope detected using the analytic signal calculated using wavelet based method is shown in Figure 6 for signal 1 and Figure 8 for signal 2 respectively.
The envelope detected using analytic signal calculated using Hilbert based method is shown in Figure 5 for signal 1 and Figure 7 for signal 2 respectively.

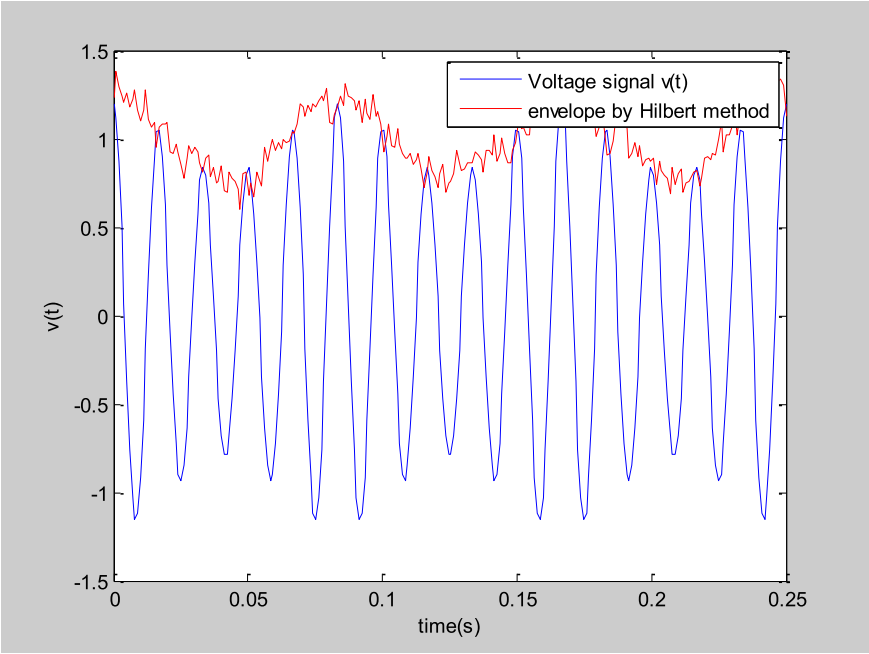

Figure 5: Envelope detection by Hilbert transform Case 1(SINGLE LFB VOLTAGE SIGNAL)

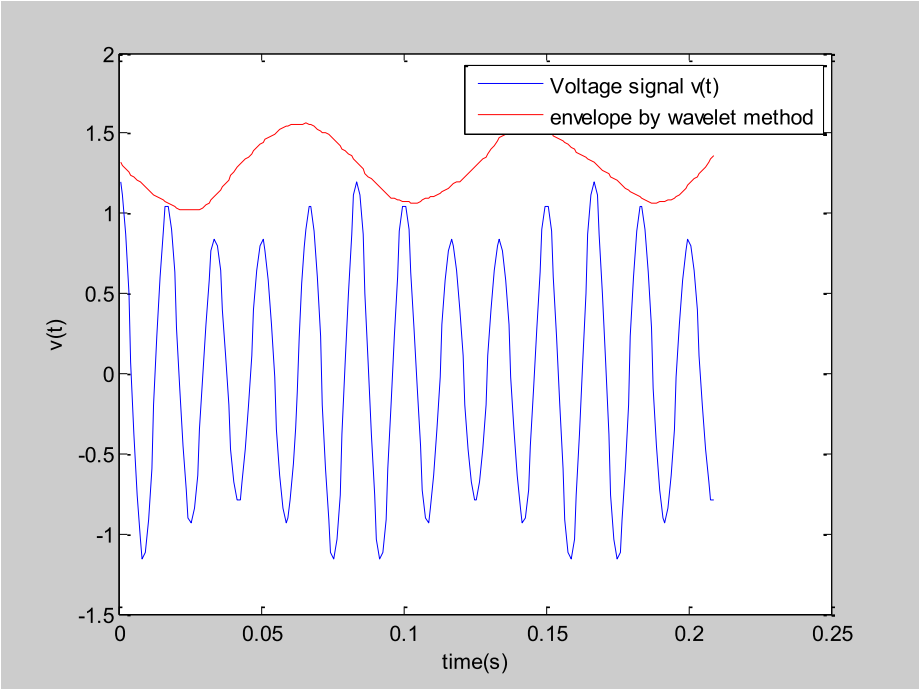

Figure 6: Envelope detection by wavelet transform Case 1(SINGLE LFB VOLTAGE SIGNAL)

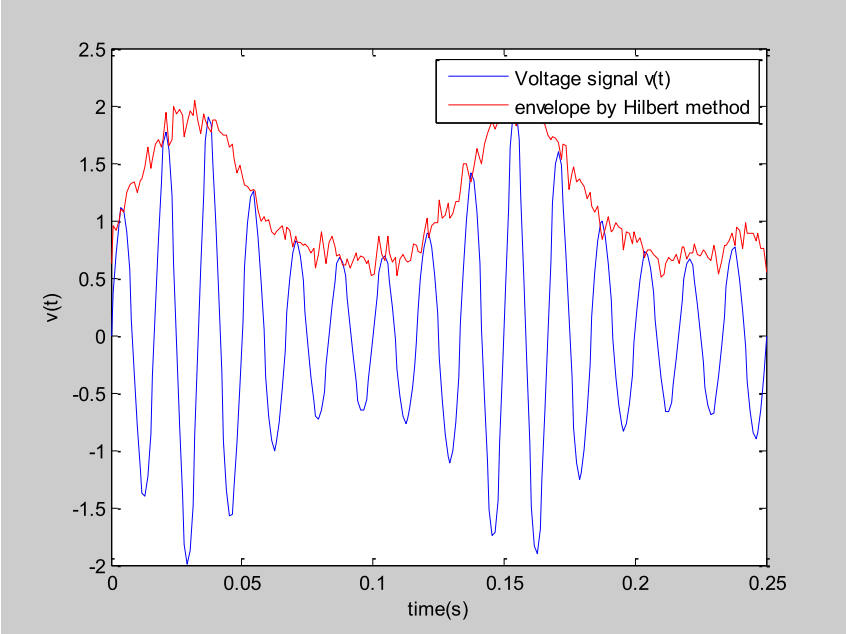

Figure 7: Envelope detection by Hilbert transform Case 2(WFB CURRENT SIGNAL)

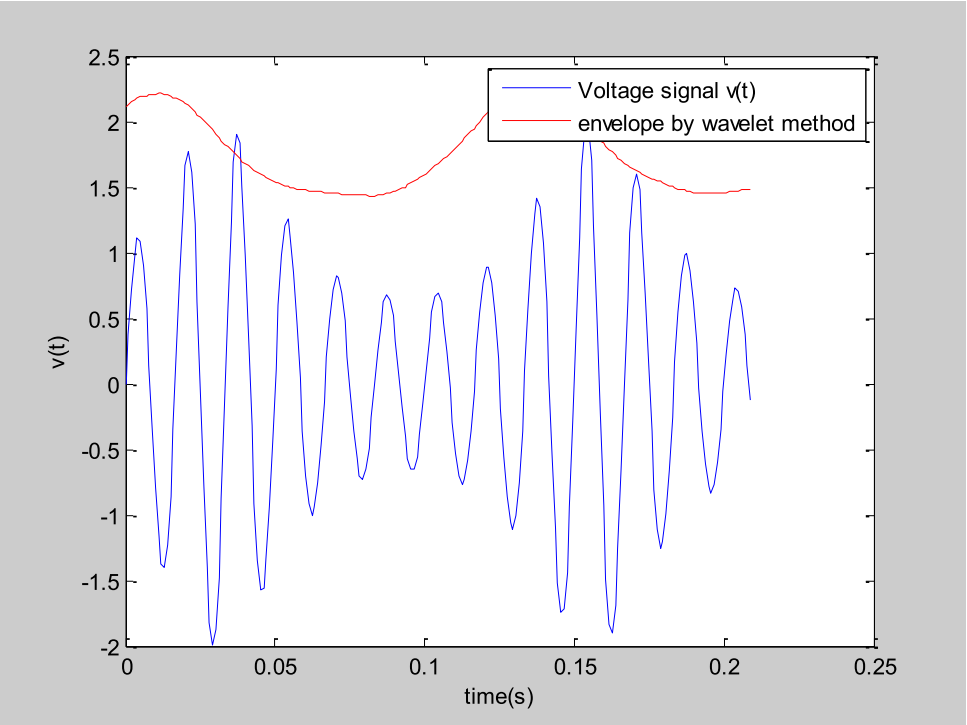

Figure 8: Envelope detection by wavelet transform Case 2(WFB CURRENT SIGNAL)

Analytic signal method	Signal to Noise Ratio (SNR) (dB)	
	Case(1)	Case (2)
Hilbert transform	22.5614	23.4955
wavelet transform	25.3275	26.6894

Table III: Comparison between SNR values for Hilbert transform and wavelet transform

Comparison: The envelope detected by the analytic signal using Hilbert transform has signal to noise ratio (SNR) equal to 22.5614 dB while envelope detected by analytic signal using wavelet transform has SNR equal to 25.3275 dB in the presence of 20 dB AWGN for the signal of case (1). The SNR value has been improved by 3dB or 2 times (3dB= 10log2) using wavelet transform based analytic signal as compared to the Hilbert transform based analytic signal. Similarly, for case (2), the SNR improved by 3dB using wavelet transform as compared to Hilbert transform method of analytic signal calculation.

5.2 Computation of Amplitude, Phase, and Frequency Modulations using Analytic Signal

This section presents simulation of AM-FM decomposition when the modulation index of AM is greater than one. We used $\mathrm{MATLAB\ 7.10.0(R2010a)}$ for this purpose. We applied the wavelet transform based method to find the analytic signal of the input waveform. Then, the square of the analytic signal is calculated. Using equation (4.5) and (4.9), bipolar amplitude modulated signal and smooth phase modulation has been constructed.

5.2.1 Simulation

We implemented AM-FM decomposition on a simulated wideband AM-FM signal given as:

$$x(t) = (1 + 1.5\cos(\omega_1 t))\cos(\omega_0 t + 0.5\cos(\omega_2 t)) + w(t)$$

The above signal is sampled at frequency of 48 kHz and the angular frequencies used are $\omega_1 = 40\pi, \omega_2 = 120\pi, \text{and } \omega_0 = 10^4\pi$ radians per second respectively; $w(t)$ is the additive white Gaussian noise of 20 dB SNR. The signal x(t) is passed through a Hamming window of length equal to the size of the signal. According to the conventional definitions of AM-FM decomposition as mentioned in equation (3.33), the resultant amplitude, phase and frequency modulation are shown in Figure 9. It is clear from Figure 9 that the conventional definitions are not able to retain the zero crossings of AM, also the corresponding FM consists of impulses at places where AM has zero crossings.

5.2.2 Analytic Signal Construction

We used wavelet transform based analytic signal to calculate the instantaneous parameter for AM/FM decomposition for over-modulated AM signal and compared the decomposition result using instantaneous parameters using Hilbert transform.

The analytic signal of the input signal $x(t)$ can be calculated using wavelet transform [3]. Equation (3.22) and (3.23) are used for this purpose.
We used wavelet function $g(t) = e^{jmt}\ e^{-\frac{1}{2}[(\sqrt{2}\,\sigma m/2\pi\tau)t]^2}$. The parameters used are m=28.28, $\sigma = 5$, $\tau = 4$, a=32, b=41.

The analytic signal calculated by wavelet transform is squared and equation (4.5) and (4.9) is applied. The resultant AM, FM and PM calculated using Hilbert transform is shown in Figure 10 and AM, FM and PM calculated using wavelet transform is shown in Figure 11 respectively. It is clear from Figure 10 and 11 that the wavelet transform based AM is able to retain its polarity while, the Hilbert transform based AM have distortions. The output

signal to noise ratio (SNR) for the amplitude modulation and the mean square error (MSE) with respect to the theoretical frequency is also calculated as shown in Table IV. It is clear from Table IV that wavelet transform has 3 dB higher noise reduction in AM as compared to the Hilbert transform. Frequency estimation using wavelet transform based analytic signal has lower mean square error as compared to the frequency estimation calculated using Hilbert transform.

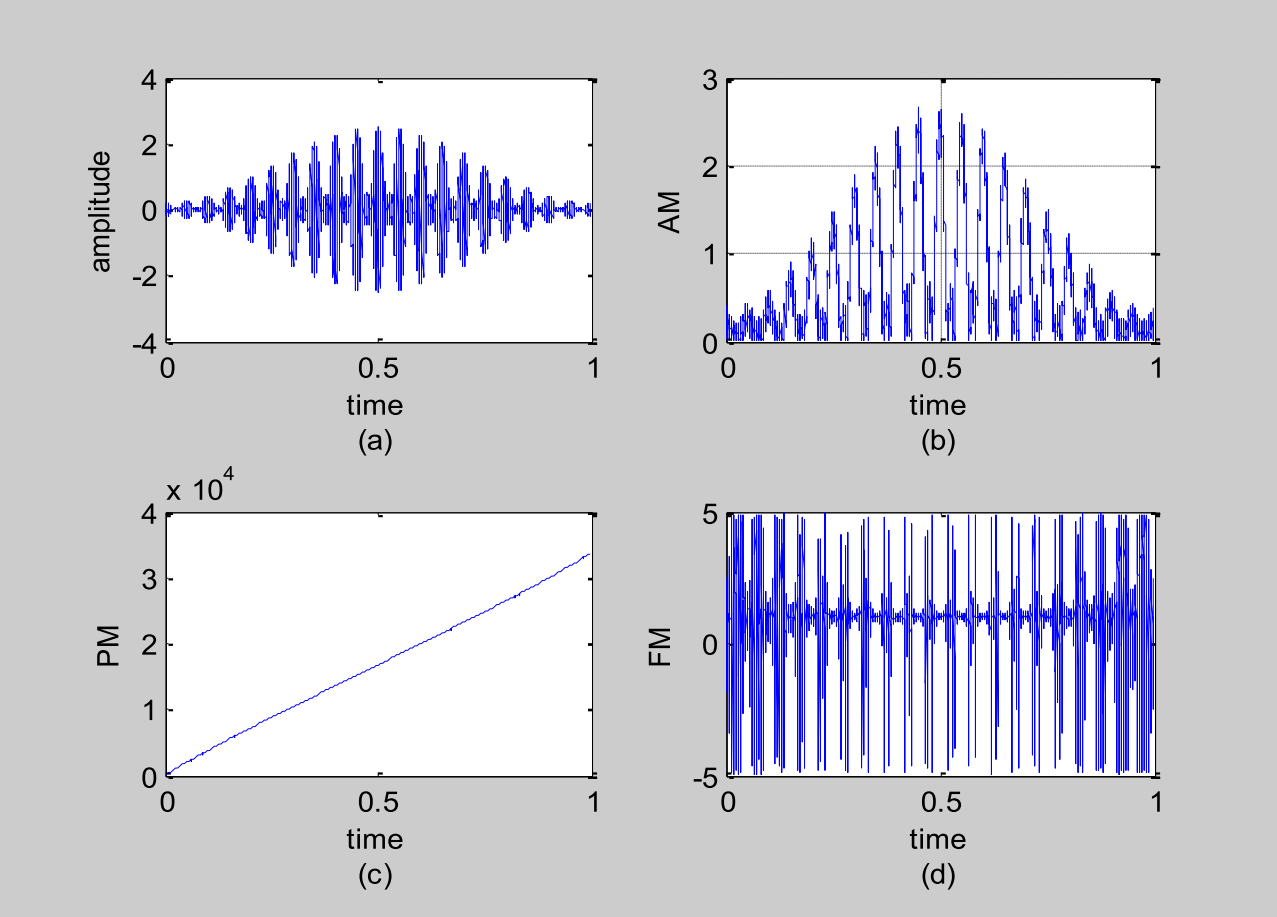

Figure 9: Decomposition of over-modulated AM-FM signal according to conventional definitions: (a) Signal (b) AM (c) PM (d) FM

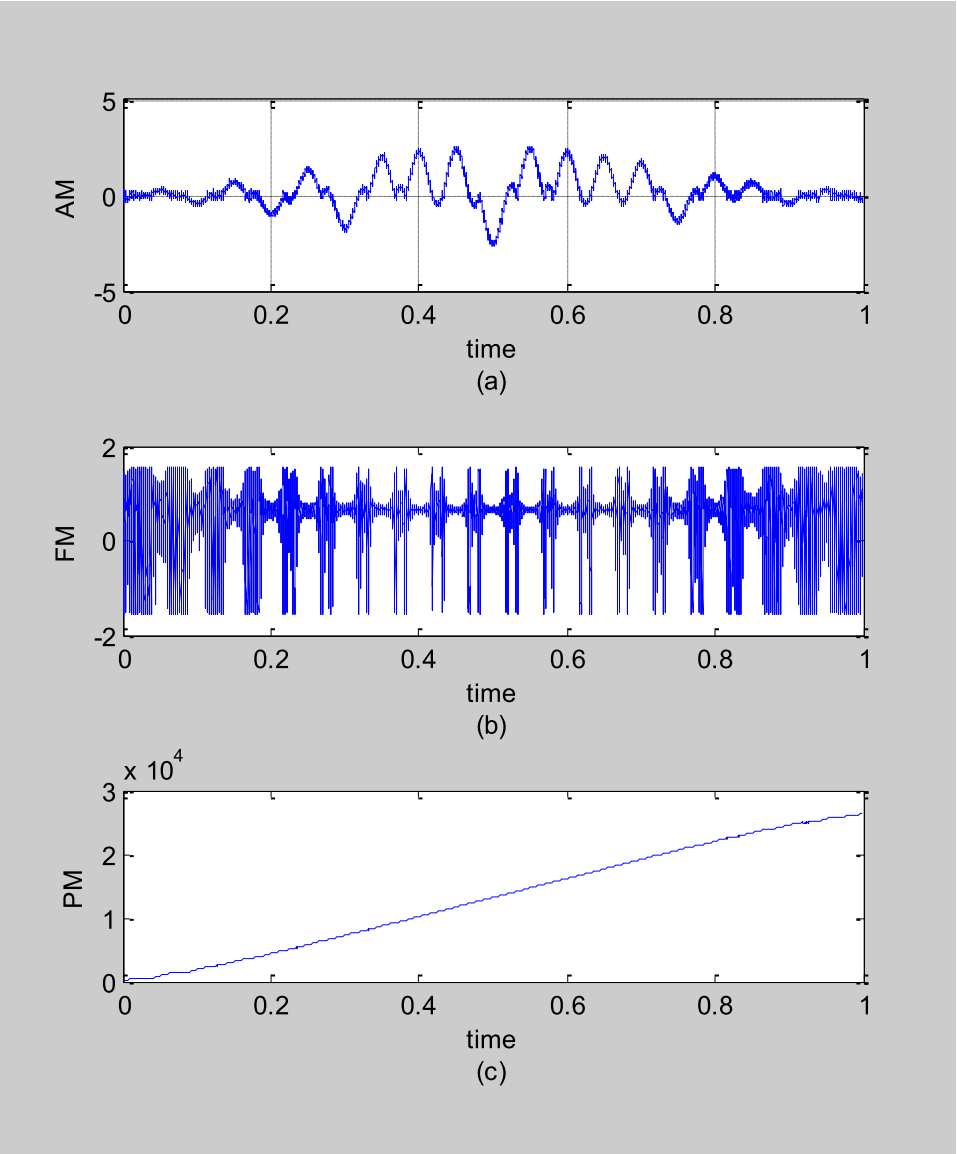

Figure 10: Decomposition results of analytic signal by Hilbert transform: (a) AM (b) FM (c) PM

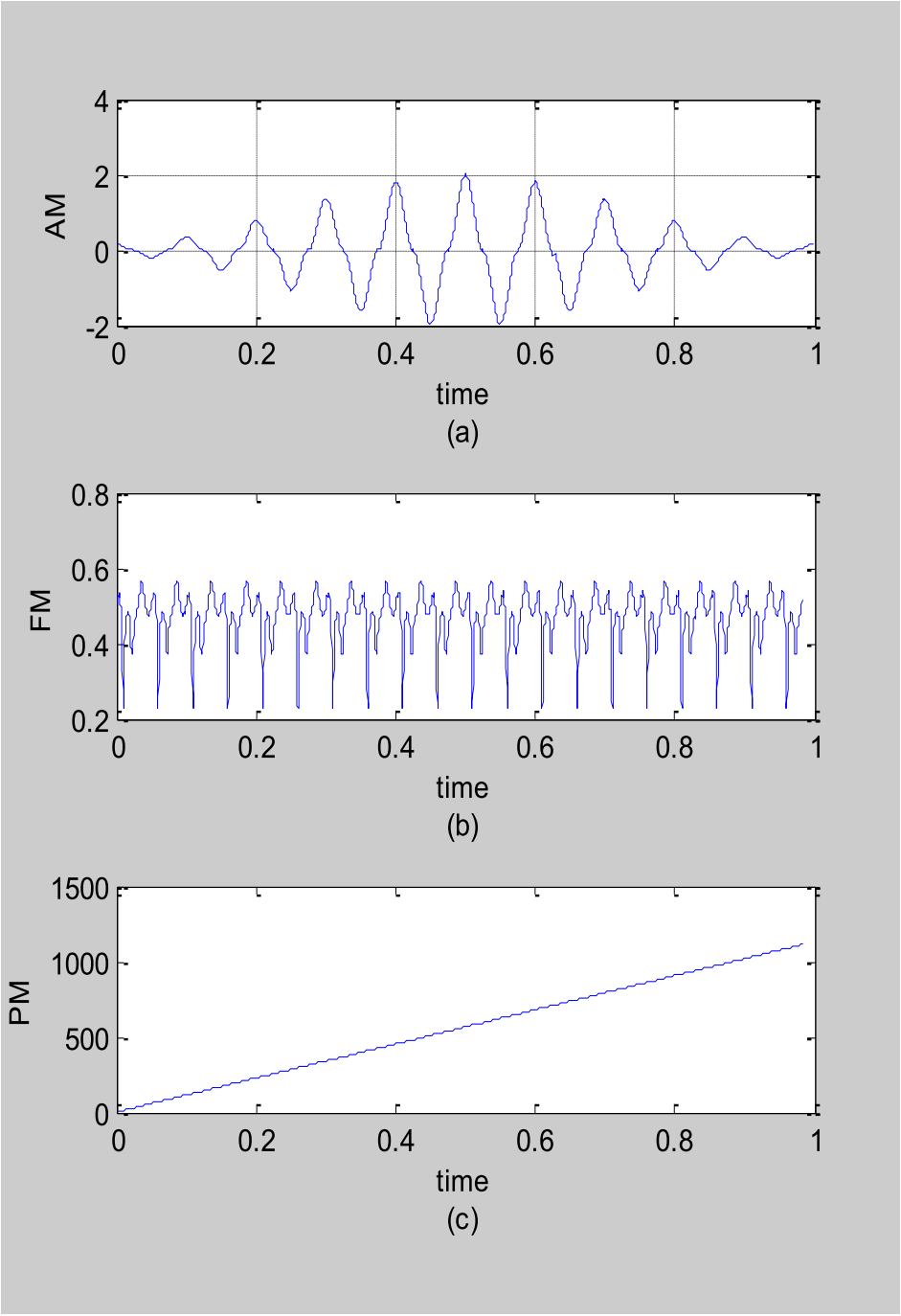

Figure 11: Decomposition results of analytic signal by wavelet transform (a) AM (b) FM (c) PM

	Signal to noise ratio (SNR): (dB)	Mean square error (MSE):
Hilbert transform	23.0393	0.8468
wavelet transform	26.59	0.0385

Table IV: SNR and MSE for decomposition using Hilbert transform method and wavelet transform method

CHAPTER 6: CONCLUSION AND FUTURE SCOPE

We described a model that characterizes time varying spatial signals and aimed to find out the instantaneous attributes of the signal. One such attribute was voltage flicker envelope detection. Here we derived the envelope of the voltage signal using the analytic signal constructed using the wavelet transform and a comparison has been made with the analytic signal using Hilbert transform. The SNR of the detected signal by wavelet transform based analytic signal was found 3 dB higher than that of Hilbert transform. The simulations were done in the presence of additive white Gaussian noise of 20 dB. Simulation results show that the voltage envelope detection using analytic signal by wavelet transform performs better in terms of noise reduction compared to the analytic signal using Hilbert transform. We also performed AM-FM decomposition analysis in the case when the corresponding amplitude modulated component is over-modulated. The instantaneous amplitude was calculated by the analytic signal via wavelet transform which also gives SNR improvement of 3 dB while keeping the AM bipolar and the mean square error for the frequency component was also found to be improved as compared to the analytic signal using Hilbert transform.

Future Scope:
Different wavelet methods can be used for denoising of signals before the implementation of analytic signal using wavelet transform.

REFERNCES

[1] E. A. Feilat, "Detection of voltage envelope using Prony analysis-Hilbert transform method", *IEEE Trans. Power Del.*, vol. 21, no. 4, pp. 2091-2093, Oct. 2006.

[2] A. Venkitaraman, C. S. Seelamantula, "On Computing Amplitude, Phase, and Frequency Modulations Using a Vector Interpretation of the Analytic Signal", *IEEE Signal Processing Letters* , vol. 20, no. 12, pp. 1187 – 1190, Dec. 2013.

[3] Gao Jinhuai, Dong Xiaolong, and Wang Wenbing, et al, "Instantaneous parameters extraction via wavelet transform," *IEEE Trans on Geoscience and Remote Sensing*, vol. 37, no. 2, pp. 867-870, March 1999.

[4] T. Tayjasanant, W. Wang, C. Li, and W. Xu, "Interharmonics-flicker curves," *IEEE Trans. Power Del.*, vol. 20, no. 2, pp. 1017–1024, Apr. 2005.

[5] M. Sun and R. J. Sclabassi, "Discrete-time instantaneous frequency and its computation," *IEEE Trans. Signal Processing*, vol. 41, no. 5, pp. 1867–1900, Nov. 1993.

[6] L. Mandel, "Interpretation of instantaneous frequencies," *Amer. J. Phys.*, vol. 42, pp. 840–846, 1974.

[7] Q. Li and L. E. Atlas, "Over-modulated AM-FM decomposition," in *Proc. SPIE* , vol. 5559, pp. 172–183. 2004

[8] M. Grimaldi, F. Cummins, "Speaker Identification Using Instantaneous Frequencies", *IEEE Trans. Audio Speech and Language Processing*, vol. 16, no. 6, pp. 1097-1111, Aug. 2008.

[9] A. Venkitaraman, C.S. Seelamantula, "Binaural signal processing motivated generalized analytic signal construction and AM–FM demodulation". *IEEE/ACM Trans. Audio Speech Lang. Processing*, vol. 22, no. 6, pp. 1023-1036, April 2014

[10] Parasuraman Sumath , Ksh Milan Singh, " Sliding discrete Fourier transform-based mono-component amplitude modulation–frequency modulation signal decomposition ", *IET Communications*, vol. 9, no. 9, pp. 1221-1229, July 2015.

[11] Haricharan Aragonda , Chandra Sekhar Seelamantula, **"**Demodulation of Narrowband Speech Spectrograms Using the Riesz Transform**"** *IEEE/ACM Transactions on Audio, Speech, and Language Processing*, vol. 23, no. 11, pp. 1824-1834, Nov. 2015

[12] Iman. Sadinezhad, V. G. Agelidis, "Frequency adaptive least-squares-Kalman technique for real-time voltage envelope and flicker estimation", *IEEE Trans. Ind. Electron.*, vol. 59, no. 8, pp. 3330-3341, Aug. 2012

[13] W. X. Yao, Q. Tang, Z. S. Teng, Y. P. Gao, H. Wen, "Fast S-transform for time-varying voltage flicker analysis", *IEEE Trans. Instrum. Meas.*, vol. 63, no. 1, pp. 72-79, Jan. 2014

[14] Feng Li, Yunpeng Gao, Yijia Cao, Reza Iravani **"**Improved Teager Energy Operator and Improved Chirp-Z Transform for Parameter Estimation of Voltage Flicker" *IEEE Trans. Power Del.*, vol. 31, no. 1, pp. 245-253, Feb. 2016.

[15] A. Dejamkhooy, A. Dastfan, "Modeling and forecasting non-stationary voltage fluctuation based on grey system theory", *IEEE Trans. Power Del.*, vol. 32, no. 3, pp. 1212-1219, June 2017.

[16] King, F.W., “Hilbert Transforms Volume 1”, Cambridge University Press, Cambridge, 2009.

[17] Kunio Takaya, “Digital Signal Processing Electrical Engineering EE-880”, University of Saskatchewan, 2004.

[18] Mathias Johansson, M.Sc. thesis, “The Hilbert transform”, VaxJo University, 1999.

[19] Easy Fourier Analysis, “Signal processing & simulation newsletter”, Available at: http://www.complextoreal.com/tcomplex.htm Accessed April 2006.

[20] https://en.wikipedia.org/wiki/Gibbs_phenomenon

[21] C. S. Burrus, R. A. Gopinath, and H. Guo, Introduction to wavelets and wavelet transforms : a primer. Upper Saddle River, N.J.: Prentice Hall, 1998.

[22] W. L. Briggs and V. E. Henson, The DFT : an owner's manual for the discrete Fourier transform. Philadelphia: Society for Industrial and Applied Mathematics, 1995.

[23] N. H. Ricker, "The form and nature of seismic waves and the structure of seismograms," *Geophysics,* vol. 5, no. 4, pp. 348-366, Oct. 1940.

[24] B. B. Hubbard, “The world according to wavelets: the story of a mathematical technique in the making”. 2nd Ed. A. K. Peters, Wellesley MA, 1998

[25] D. Gabor, "Theory of communication- Part 3: Frequency compression and expansion", *J. Inst. Elect. Eng. Part III Radio Commun.*, vol. 93, no. 26, pp. 445-457, 1946

[26] J. Y. Stein, “Digital signal processing: a computer science perspective” New York: Wiley, 2000.

[27] A. Graps, "An introduction to wavelets," *IEEE Comput. Sci. Eng.*, vol. 2, no. 2, pp. 50-61, Summer 1995

[28] C. Valens, “ A Really Friendly Guide to Wavelets”, 1999.

[29] A. Grossmann, J. Morlet, "Decomposition of hardy functions into square integrable wavelets of constant shape," *SIAM Journal on Mathematical Analysis*, vol. 15, no.4, pp. 723-736, 1984.

[30] J. Lin and L. Qu, “Feature extraction based on morlet wavelet and its application for mechanical fault diagnosis,” *Journal of Sound and Vibration*, vol. 234, no. 1, pp. 135–148, Jun. 2000.

[31] G. Jinghuai, W. Wenbing, Z. Guangming, P. Yuhua, and W. Yugui,” On the choice of wavelet functions in seismic data processing,” *Acta Geophys. Sinica*, vol. 39, pp. 392–400, 1996

[32] Rasmussen, Henrik O. "The Wavelet Gibbs Phenomenon." in "*Wavelets, Fractals and Fourier Transforms*", Eds M. Farge *et al*., Clarendon Press, Oxford, 1993.

[33] Kelly, Susan E. "Gibbs Phenomenon for Wavelets." Applied and Computational Harmonic Analysis 3, 1995.

[34] G. Jinghuai, W. Wenbing, and Z. Guangming, "Wavelet transform and instantaneous attributes analysis of a signal," *Acta Geophys. Sinica*, vol. 40, pp. 821–832, 1997.

[35] K. Saberi and E. R. Hafter, "A common neural code for frequency- and amplitude-modulated sounds," *Nature*, vol. 374, pp. 537-9, 1995

[36] R. McEachern, "How the ear really works,", *Proceedings IEEE-SP International Symposium, Time-Frequency and Time-Scale Analysis, 1992*., Victoria, BC, Canada, 1992.

[37] Z. M. Smith, B. Delgutte, and A. J. Oxenham, "Chimaeric sounds reveal dichotomies in auditory perception," Nature, vol. 416, pp. 87-90, 2002.

[38] L. E. Atlas, Q. Li, and J. K. Thompson, "Homomorphic modulation spectra," *IEEE ICASSP '04,* Motreal, Canada, 2004.

[39] L. E. Atlas and M. S. Vinton, "Modulation frequency and efficient audio coding," *Proc. SPIE The International Society for Optical Engineering,* 2001.

[40] B. Picinbono, "On instantaneous amplitude and phase of signals," *IEEE Transactions on Signal Processing*, vol. 45, no. 3, pp. 552-560, March 1997.

[41] L. Cohen, P. Loughlin, D. Vakman, "On an ambiguity in the definition of the amplitude and phase of a signal", *Elsevier Signal Process.*, vol. 79, pp. 301-307, Jun. 1999.

[42] J. F. Hauer, C. J. Demeure, and L. L. Scharf, "Initial Results in Prony Analysis of Power System Response Signals," *IEEE Trans. Power Systems*, vol. 5, no. 1, pp. 80-89, Feb. 1990.

[43] O. Chaari, P. Bastard, and M. Meunier, "Prony's method: An Efficient Tool for the Analysis of Earth Fault Currents in Petersen-coil-protected Networks", *IEEE Trans. On Power Delivery*, ,vol. 10, no. 3, pp. 1234-1242. July 1995

[44] https://en.wikipedia.org/wiki/Prony%27s_method

[45] A. W. Lohmann, D. Mendlovic, and Z. Zalevsky, "Fractional Hilbert transform," *Opt. Lett.*, vol. 21, no. 4, pp. 281–283, Feb. 1996.